Fall 2018

Comparative toxicology of NiO and $Ni(OH)_2$ nanoparticles

Melissa Hope Cambre

Department:

COMPARATIVE TOXICOLOGY OF NiO AND $Ni(OH)_2$ NANOPARTICLES

by

MELISSA HOPE CAMBRE

A THESIS

Presented to the Faculty of the Graduate School of the

MISSOURI UNIVERSITY OF SCIENCE AND TECHNOLOGY

In Partial Fulfillment of the Requirements for the Degree

MASTER OF SCIENCE IN APPLIED AND ENVIRONMENTAL BIOLOGY

2018

Approved by

Yue-Wern Huang, Advisor
Chen Hou
Paul Nam

PUBLICATION THESIS OPTION

This thesis consists of the following two articles.

Paper I, pages 2-26, have been published by the International Journal of Molecular Sciences

Paper II, pages 27-58, are intended for submission to Toxicology Letters.

ABSTRACT

Understanding the potential toxicity of nanoparticles (NPs) is important to ensure that these new products do not impose harmful effects to human and environmental health. Paper I is a literature review in which we discuss characteristics of nanomaterials, with an emphasis on transition metal oxide nanoparticles that influence cytotoxicity. Identification of those properties may lead to the design of more efficient and safer nanosized products for various industrial purposes and provide guidance for assessment of human and environmental health risk. We then investigate biochemical and molecular mechanisms of cytotoxicity that include oxidative stress-induced cellular events and alteration of the pathways pertaining to intracellular calcium homeostasis. All the stresses lead to cell injuries and death. Furthermore, as exposure to nanoparticles results in deregulation of the cell cycle (i.e., interfering with cell proliferation). Paper II is about our original research in which we evaluated the differential cytotoxicity between nickel oxide (NiO) and nickel hydroxide $Ni(OH)_2$ in human bronchoalveolar carcinoma (A549) and human hepatocellular carcinoma (HepG2) cell lines. Cellular viability assays revealed cell line-specific cytotoxicity in which nickel NPs were only toxic to A549 cells. Time-, concentration-, and particle-specific viability was observed in A549 cells. NP-induced oxidative stress triggered subsequent dissipation of mitochondrial membrane potential and induction of caspase-3 enzyme activity. The subsequent apoptotic events lead to reduction in cell number, though the contribution of necrosis to cell viability is unknown. In addition to cell death, suppression of cell proliferation contributes to play an essential role in regulating cell number. Collectively, the observed cell viability is a function of cell death and suppression of proliferation.

ACKNOWLEDGMENTS

I would like to thank my advisor, Dr. Yue-Wern Huang for all of his guidance in the completion of my study. I appreciate all the time he has dedicated to guiding and supporting me with my writing and data collection. I would also like to thank Dr. Chen Hou and Dr. Paul Nam for taking the time to serve on my committee.

I would like to thank Mr. Larry Toliver for guiding me in my early study. He taught me several experimental procedures and problem-solving skills that served useful throughout my graduate career. I would also like to give a special thanks to Mr. Bolin Wang and Mr. Lucas Harper for their assistance in my study.

TABLE OF CONTENTS

Page

LIST OF ILLUSTRATIONS

Page

Paper I

Paper II

LIST OF TABLES

Page

Paper I

Paper II

SECTION

1. INTRODUCTION

Nanoparticles have become increasingly popular in industrial uses for their unique and useful properties. This increase in use necessitates the need to assess the safety of these nanoparticles for human and environmental health. Paper one explores some of the specific properties that have made certain nanoparticles produce more toxic effects than others. The biochemical and molecular mechanisms of cytotoxicity are then explored, with an emphasis on the mechanisms of cell cycle alteration. Overall, viability is thought to be a function of the suppression of proliferation and cell killing. Paper two explores the specific differential toxicity between NiO and $Ni(OH)_2$. Differences in viability upon nanoparticle exposure are thought to be cell line-, time-, concentration-, and particle-dependent. Various mechanisms responsible for viability are investigated including induction of oxidative stress, dissipation of mitochondrial membrane potential, and induction of caspase-3 enzymatic activity. Alterations in cell cycle, changes in proliferation rate, and induction of apoptosis are also delineated. In summary, cytotoxicity is mediated by oxidative stress-mediated cell death and suppression of proliferation.

PAPER

I. THE TOXICITY OF NANOPARTICLES DEPENDS ON MULTIPLE MOLECULAR AND PHYSICOCHEMICAL MECHANISMS

Yue-Wern Huang[1]*, Melissa Cambre[1] and Han-Jung Lee[2]
[1]Department of Biological Sciences, Missouri University of Science and Technology, Rolla, 143 Schrenk Hall, 1870 Miner Circle, Rolla, MO 65409, USA; mhcxv8@mst.edu
[2]Department of Natural Resources and Environmental Studies, National Dong Hwa University, Hualien 97401, Taiwan; hjlee@mail.ndhu.edu.tw
*Correspondence: huangy@mst.edu; Tel.: +1-573-341-6589; Fax: +1-573-341- 4821
Received: 28 September 2017; Accepted: 11 December 2017; Published: 13 December 2017

ABSTRACT

Nanotechnology is an emerging discipline that studies matters at the nanoscale level. Eventually, the goal is to manipulate matters at the atomic level to serve mankind. One growing area in nanotechnology is biomedical applications, which involve disease management and the discovery of basic biological principles. In this review, we discuss characteristics of nanomaterials, with an emphasis on transition metal oxide nanoparticles that influence cytotoxicity. Identification of those properties may lead to the design of more efficient and safer nanosized products for various industrial purposes and provide guidance for assessment of human and environmental health risk. We then investigate biochemical and molecular mechanisms of cytotoxicity that include oxidative stress-induced cellular events and alteration of the pathways pertaining to intracellular calcium

homeostasis. All the stresses lead to cell injuries and death. Furthermore, as exposure to nanoparticles results in deregulation of the cell cycle (i.e., interfering with cell proliferation), the change in cell number is a function of cell killing and the suppression of cell proliferation. Collectively, the review article provides insights into the complexity of nanotoxicology.

Keywords: nanoparticle; toxicity; physicochemical property; cell proliferation; calcium homeostasis; oxidative stress

1. INTRODUCTION

Nanoscience is the study of the control of matters at the atomic and molecular scale. Nanomaterials are materials that have at least one dimension in the range of 1–100 nm. In addition to discovering fundamental principles and advancing knowledge in nanoscience, nanomaterials have a wide spectrum of applications in our society. Table 1 summarizes the industrial applications of transition metal oxide nanoparticles [1–24]. Some engineered nanomaterials are being used in products with direct exposure to humans. For example, TiO_2 nanoparticles are used in food coloring, cosmetics, skin care products, and tattoo pigment [1–7]. Fe_2O_3 nanoparticles are used in the final polish on metallic jewelry. ZnO nanoparticles are added to many products including cotton fabric, food packaging, and rubber for its deodorizing and antibacterial properties [18–20]. Engineered nanomaterials also show promise for applications in life science and biomedical utility such as cellular receptor trafficking, delivery of biologically active molecules, disease staging and therapeutic planning, and nanoelectronic biosensors

[25,26]. For instance, nanoparticles incorporated with targeting ligands can enter cancer cells, where they can release therapeutic drugs [25]. This could decrease the amount of drug needed to treat a disease (i.e., higher therapeutic efficacy) as well as unwanted side effects (toxicity). There are more than 3000 nanoparticulate-based commercial applications. By the end of 2019, its worldwide market is estimated to be $79.8 billion [27]. As the use of engineered nanomaterials continues to grow exponentially, unintended and intended exposure may occur, leading to a greater degree of human health risk. The exposure routes may include inhalation, ingestion, skin, and injection. End-product users, occupational exposed subjects, and the general public may be at risk of adverse effects. The use of nanomaterials has significantly grown in the automotive, construction, energy, biomedical, electronic, textile, chemical, and cosmetic industries [28]. Uncovering the specific particle surface properties that cause some to be more toxic than others requires a systematic study focusing on nanoparticles similar in composition (size and morphology). Therefore, we choose to focus on transition metal oxide nanoparticles widely used in various industrial applications.

2. CHARACTERISTICS OF NANOPARTICLES THAT INFLUENCE TOXICITY

The physiochemical properties of nanoparticles influence how they interact with cells and, thus, their overall potential toxicity. Understanding these properties can lead to the development of safer nanoparticles. Recent studies have begun identifying various properties that make some nanoparticles more toxic than others. Theoretically, particle size is likely to contribute to cytotoxicity. Given the same mass, smaller nanoparticles

have a larger specific surface area (SSA) and thus more available surface area to interact with cellular components such as nucleic acids, proteins, fatty acids, and carbohydrates. The smaller size also likely makes it possible to enter the cell, causing cellular damage. In some nanoparticles, toxicity was found to be a function of both size and SSA. For instance, the size of anatase TiO_2 was shown to correlate with reactive oxygen species (ROS) production when comparing the amount of ROS production per surface area within a certain size range [29]. Particles below 10 or above 30 nm produced similar levels of ROS per surface area. However, there was a dramatic increase in ROS production per unit surface area in particles increasing from 10 to 30 nm. This information provides insight regarding the complex relationship between nanoparticle properties and nanotoxicity. Further studies are needed to determine whether a similar phenomenon applies to other forms of TiO_2 or other particles.

Particle surface charge may affect the cellular uptake of particles as well as how the particles interact with organelles and biomolecules. Consequently, particle surface charge influences cytotoxicity. According to mathematical probability and assuming particles are toxic, high particle uptake (i.e., higher bioavailability) correlates with higher toxicity. For instance, three similarly sized iron oxide particles with different charges were found to have differential toxicities on a human hepatoma cell line (BEL-7402) [30]. Oleic acid-coated Fe_3O_4, carbon-coated Fe, and Fe_3O_4 had surface charges of 4.5, 23.7, and 14.5 mV, respectively. The toxicity of the nanoparticles increased with an increase in surface charge. This suggests that the higher positive charge the nanoparticle has, the greater electrostatic interactions it has with the cell and, thus, greater endocytic uptake. Another example is that positively charged ZnO nanoparticles produce more

Table 1. Applications of transition metal oxide nanoparticles.

Elements	Oxide	Potential Application
Scandium (Sc)	Sc_2O_3	Used in high-temperature systems for its resistance to heat and thermal shock, electronic ceramics, and glass composition
Titanium (Ti) [1–7]	TiO_2	White pigment, white food coloring, cosmetic and skin care products, thickener, tattoo pigment and styptic pencils, plastics, semiconductor, solar energy conversion, solar cells, solid electrolytes, detoxification or remediation of wastewater; used in resistance-type lambda probes; can be used to cleave protein that contains the amino acid proline at the site where proline is present, and as a material in the meristor
Vanadium (V)	V_2O_5	Catalyst, a detector material in bolometers and microbolometer arrays for thermal imaging, and in the manufacture of sulfuric acid, vanadium redox batteries; preparation of bismuth vanadate ceramics for use in solid oxide fuel cells [8]
	V_2O_3	Corundum structure as an abrasive [9], antiferromagnetic with a critical temperature at 160 K [10] can change in conductivity from metallic to insulating
Chromium (Cr)	Cr_2O_3	Protection of silicon surface morphology during deep ion coupled plasma etching of silica layers; used in paints, inks, and is the precursor to the magnetic pigment chromium dioxide
	CrO_2	Magnetic tape emulsion, data tape applications
Manganese (Mn)	MnO_2	Electrochemical capacitor, as a catalyst; used in industrial water treatment plants
Iron (Fe)	Fe_2O_3	Used as contrast agents in magnetic resonance imaging, in labeling of cancerous tissues, magnetically controlled transport of pharmaceuticals, localized thermotherapy, preparation of ferrofluids [11,12], final polish on metallic jewelry and lenses, as a cosmetic
	FeO	Tattoo inks
	Fe_3O_4	MRI scanning [13], as a catalyst in the Haber process and in the water gas shift reaction [14], and as a black pigment [15]
Cobalt (Co)	Co_2O_3	Catalyst; for studying the redox and electron transfer properties of biomolecules; can immobilize protein
	CoO	Blue colored glazes and enamels, producing cobalt(II) salts
Nickel (Ni)	NiO	In ceramic structures, materials for temperature or gas sensors, nanowires and nanofibers, active optical filters, counter electrodes
	Ni_2O_3	Electrolyte in nickel plating solutions; an oxygen donor in auto emission catalysts; forms nickel molybdate, anodizing aluminum, conductive nickel zinc ferrites; in glass frit for porcelain enamel; thermistors, varistors, cermets, and resistance heating element
Copper (Cu)	CuO	Burning rate catalyst, superconducting materials, thermoelectric materials, catalysts, sensing materials, glass, ceramics, ceramic resisters, magnetic storage media, gas sensors, near infrared tilters, photoconductive applications, photothermal applications, semiconductors, solar energy transformation [16]; can be used to safely dispose of hazardous materials [17]
	Cu_2O	Pigment, fungicide, antifouling agent for marine paints, semiconductor
Zinc (Zn)	ZnO	Added to cotton fabric, rubber, food packaging [18–20], cigarettes [21], field emitters [22], nanorod sensors; Applications in laser diodes and light emitting diodes (LEDs), a biomimic membrane to immobilize and modify biomolecules [23]; increased mechanical stress of textile fibers [24]

cytotoxic effects in A549 cells than negatively charged particles of a similar shape and size [31]. The phenomenon can be explained, in part, in the context of cellular membrane composition. Glycosaminoglycans are abundant on the mammalian cell surface. These molecules are negatively charged and therefore are likely to interact electrostatically with positively charged nanoparticles [32]. The longer and the more the electrostatic interactions, the more likely nanoparticles are to be internalized [33]. The same is true in positively charged nanoparticles interacting with negatively charged DNA, leading to DNA damage.

Shape also affects levels of toxicity. Amorphous TiO_2 was found to generate more ROS than anatase or rutile of a similar size, with rutile TiO_2 causing the least amount of ROS [29]. It is likely that amorphous TiO_2 has more surface defects, and therefore active sites that are capable of causing ROS. The anatase form of TiO_2 was also significantly more toxic to PC12 cells than the rutile form even though the particles are similar in size and chemical make-up [34]. Rod-shaped Fe_2O_3 nanoparticles were found to produce much higher cytotoxic responses than sphere-shaped Fe_2O_3 nanoparticles in a murine macrophage cell line (RAW 264.7), including higher levels of lactate dehydrogenase (LDH) leakage, inflammatory response, ROS production, and necrosis [35]. Finally, rod-shaped CeO_2 nanoparticles were found to produce more toxic effects in RAW 264.7 cells than octahedron or cubic particles [36]. Rod-shaped CeO2 nanoparticles produced significant lactate dehydrogenase LDH release and tumor necrosis factor alpha (TNF) in RAW 264.7 cells, while neither octahedron nor cubic produced significant responses. Why the physical shape of a nanoparticle influences cytotoxicity remains to be elucidated.

Though the above studies and others have contributed to the understanding of how and why properties of nanoparticles mediate toxicity, a more systematic approach can even further advance our knowledge in this regard. Our laboratory systematically selected seven oxides of transition metals (Ti, Cr, Mn, Fe, Ni, Cu, and Zn) from the fourth period of the periodic table of elements [33]. Four properties of nanomaterials were tested: particle surface charge, available binding site on particle surface, particle metal dissolution, and band-gap energy (Figure 1). Particle surface charge was determined by point-of-zero charge (PZC). We used X-ray photoelectron spectroscopy (XPS) to measure available binding site on particle surface. Metal ions released from oxides were analyzed with inductively coupled plasma mass spectrometry (ICP-MS). Finally, bad-gap energy, which is the energy difference between the top of the valence band and the bottom of the conduction band in insulators and semiconductors, was spectroscopically determined. We found that (1) as the atomic number of the element increases, cytotoxicity increases; and (2) alteration of cell viability is a function of particle surface charge, available binding site on a particle surface, and particle metal dissolution, but not of band-gap energy.

3. BIOCHEMICAL AND MOLECULAR MECHANISMS OF CYTOTOXICITY

There have been intensive nanotoxicological studies since the turn of the century [37–40]. Mechanisms of in vivo nanotoxicity are numerous. They may include, but not limited to, pulmonary and systemic inflammation, platelet activation, altered heart rate variability, and vasomotor dysfunction [41]. While in vivo studies provide critical

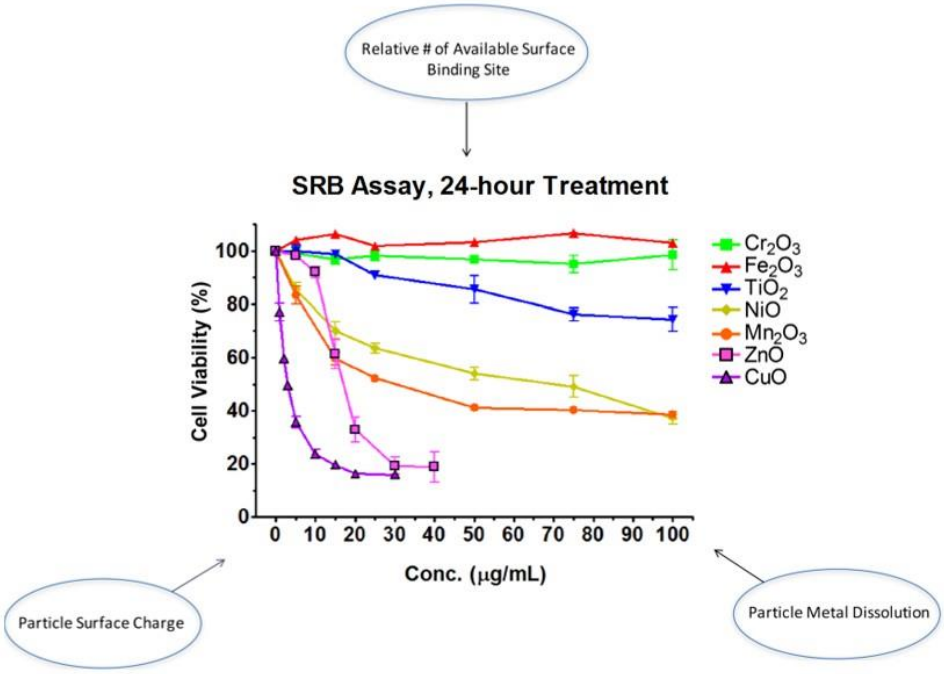

Figure 1. Certain physicochemical parameters of transition metal oxide nanomaterials influence toxicity.

information for risk assessment, in vitro studies help us understand molecular and biochemical mechanisms of nanotoxicity and give insight into the physicochemical properties of nanomaterials that contribute to the toxicity. For instance, metal oxide nanoparticles can elevate the level of oxidative stress (OS) via production of reactive oxygen species (ROS; e.g., $O_2^{\bullet -}$, $OH^{\bullet}$, H_2O_2) in a variety of ways [42]. These high-energy species can attack lipids, nucleic acids, proteins, and other essential biomolecules. The consequential damage includes damage to mitochondrial structure, depolarization of mitochondrial membrane, impairment of the electron transport chain, and the activation of an NADPH-like system [43]. Our laboratory has focused on delineating multiple biochemical and molecular mechanisms of toxicity induced by exposure to a variety of

nanoparticles (Figure 2). The nanoparticles tested can elevate cellular OS, which is manifested in reduced levels of the antioxidants GSH and α-tocopherol [44,45]. This leads to cellular injury or death via altered signaling pathways. Compromise of cell membrane integrity is detected via release of LDH from the cell [44,45]. DNA injuries, including double-strand and single-strand breakages, are identified according to the comet assay [46]. DNA damage can lead to cell cycle arrest or apoptosis. An oxidative stress and antioxidant defense microarray assay found alterations in the expression of four genes that are involved in apoptosis and OS responses: BNIP, PRDX3, PRNP, and TXRND1 [47]. Membrane depolarization occurs in cells treated with aluminum oxide (AL_2O_3) and cerium oxide (CeO_2) [48].

In addition to OS, we observed nanoparticle-induced perturbation of intracellular calcium [Ca^{2+}] in homeostasis, which can be attributed to several molecular actions and is associated with metabolic and energetic imbalance as well as cellular dysfunction [47] (Figure 2). Zinc oxide (ZnO) nanoparticles increase $[Ca^{2+}]_{in}$. The moderation of this increase by nifedipine suggests that a portion of this increase reflects an influx of extracellular calcium. Membrane disruption (e.g., by the demonstrated lipid peroxidation, malondialdehyde MDA) may also play a role in this influx. Nanomaterials disrupt store-operated calcium entry [49,50]. There exist crosstalks between intracellular $[Ca^{2+}]_{in}$ and OS, and the increases in both can be reduced by an antioxidant. Finally, while $[Ca^{2+}]_{in}$ and OS affect the activity of each other, they induce cell death by distinct pathways. These findings suggest that nanomaterials can trigger cell death via multiple pathways.

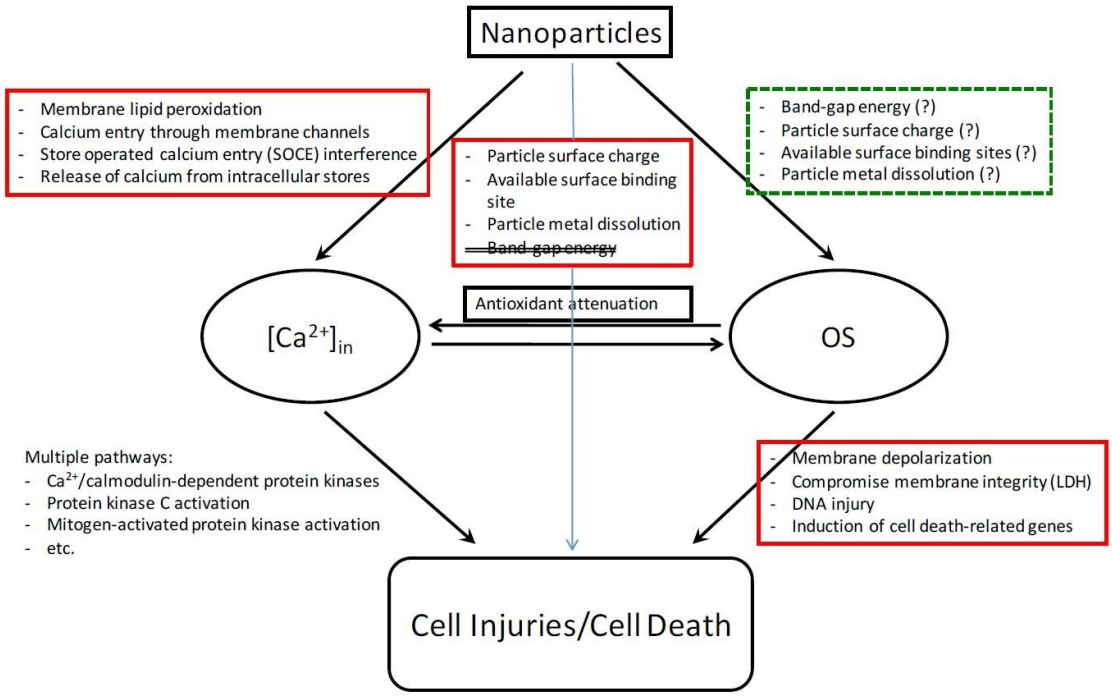

Figure 2. Multiple mechanisms of nanoparticle toxicity contribute to cell cycle deregulation and cell death. Particles used to delineate the pathways include Al_2O_3, SiO_2, CeO_2, and transition metal oxides.

Studies have shown a decrease in mitochondrial membrane potential (MMP) upon exposure to ZnO in human bronchial epithelial cells (BEAS-2B) and human alveolar adenocarcinoma cells (A549) as detected by the MitoTracker® Red CMXRos and JC-1 assay, which indicate risk of early apoptosis [51]. TiO_2 causes a loss of MMP in neuronal cells (PC12) and lung A549 cells [34,52]. Fe_3O_4 caused a loss of MMP in human mesenchymal stem cells (hMSCs) [53] and human hepatoma cells (BEL-7402) [30]. TEM images show that ZnO nanoparticles appeared to physically squeeze mitochondrial cells in HaCaT cells, likely one mechanism of mitochondrial damage [54]. Recent studies investigated protein deregulation by metal oxide nanoparticles [55]. Using circular dichroism (CD), Fourier transformed infrared spectrometry (FTIR), fluorescence

spectroscopy (FS), Raman spectroscopy (RS), and nuclear magnetic resonance (NMR), the binding of proteins to ZnO, TiO_2, SiO_2, or FeO nanoparticles can result in minor conformational changes or protein denaturation, an irreversible binding of proteins to a nanoparticle [55]. Furthermore, metal ions such as Zn^{2+} and Cu^{2+} released from ZnO and CuO can cause damage to proteins. Metal ions such as copper and zinc can inactivate certain metalloproteins by dislodging metal ions within them [56]. Another mechanism of nanotoxicity pertains to cell cycle arrest. Deregulation of cell cycle occurs in cells exposed to TiO_2, Fe_2O_3, CuO, NiO, ZnO, and Al_2O_3 [30,34,51–54,57–68] (Table 2). Cells in cell cycle arrest will either exit cell cycle arrest with potentially compromised cellular function or undergo apoptosis.

4. MECHANISMS OF CELL CYCLE ARREST

While previous studies have been focusing on alteration of cell viability, recent studies have demonstrated that a change in cell number in cytotoxicity tests reflects not just cell killing but also cell cycle arrest, which leads to a suppression of cell proliferation. Therefore, studies on cell cycle arrest aid a better understanding of the reduction of viable cells. The suppression of cell proliferation occurs when cells become arrested in one or more cell cycle phases. Cell growth can become arrested in the G_0/G_1 phase, the S phase, or the G_2/M phase. The phase in which cell growth becomes arrested is cell-type- and nanoparticle-specific [30,34,51–54,57–68]. Table 2 demonstrates various changes in cell cycle upon exposure to different nanoparticles in a variety of cell lines. Certain nanoparticles are likely to cause DNA damage, which may lead to cell cycle

arrest. Cells arrested in cell cycle will either fix the damage or accumulate too much damage and undergo apoptosis. While the underlying mechanisms in which cells become arrested in certain phases of the cell cycle vary, all cells undergoing cell cycle arrest experience a suppression of proliferation. The degree to which cells experience an inhibition of proliferation influences cell number from one generation to the next.

4.1. CELL-TYPE-DEPENDENT SUPPRESSION OF THE CELL CYCLE

Exposure of nickel oxide nanoparticle (NiONP) resulted in a significant increase in the G_0/G_1 in the BEAS-2B cell line but a significant decrease of the G_0/G_1 phase in the A549 cell line [57]. Consequently, exposure to NiONP resulted in a significant decrease in the G_2/M in the BEAS-2B cell line and a significant increase of the G_2/M phase in the A549 cell line. However, the S phase was only significantly affected in the BEAS-2B cell line. Furthermore, exposure to ZnO caused an increase in the population of cells in the G_2/M phase in A549 cells but did not affect cell cycle distribution in BEAS-2B cells. [51]. These studies demonstrate that cell cycle arrest is cell-type-specific, evidence of cellular stress activating different response pathways in different cell types.

4.2. NANOPARTICLE DEPENDENT SUPPRESSION OF CELL CYCLE

Cell cycle arrest also differs based on the type of nanoparticle. It appears that cell cycle arrest occurs most commonly in the G_2/M phase. However, arrest can also happen in the G_0/G_1 and S phases. In BEAS-2B cells, exposure to NiO caused cells to become arrested in the G_0/G_1 phase, while exposure to ZnO and Fe_2O_3 did not affect the cell cycle [51,57]. ZnO and CuO exposure resulted in arrest in the G_2/M phase, while TiO_2

exposure resulted in arrest in the S phase in HaCaT cells [54,58,62]. Al_2O_3 and Fe_3O_4 caused an increase in the sub-G_0 phase of human mesenchymal stem cells (hMSFs) [53,63]. A549 cells became arrested in the G_2/M phase upon exposure to CuO, NiO, and ZnO, but experience no change in cell cycle upon exposure to Fe_2O_3 [51,57,59,60]. One study found that TiO_2 exposure caused A549 cells to become arrested in the G0/G1 phase, while two other studies found that exposure caused arrest in the G_2/M phase [52,60,61]. This could be due to differences in TiO_2's size or other properties. Collectively, cell cycle alteration is a complex matter involving properties of both cells and particles.

4.3. CHANGES IN GENE EXPRESSION UNDERLIE THE MECHANISMS OF CELL CYCLE ARREST

Study of gene responses upon nanoparticle exposure can further enhance our understanding of the biological pathways in which nanoparticles induce cell cycle arrest. Cell cycle progression is regulated by a variety of growth factors that promote transition through various phases as well as inhibitors that prevent or decelerate transition. Exposure to nanoparticles can result in a wide array of gene expression deregulation pertaining to the cell cycle. For instance, exposure to CuO nanoparticles causes downregulation of 90 cell cycle genes [59]. Nanoparticle exposure can affect different genes in different cell lines upon exposure to the same nanoparticle. There is a cell-type-specific difference in the regulation of the cell cycle between a normal intestinal cell line NCM460 and two cancerous intestinal cell lines, DLD-1 and SW480 [69]. ZnO exposure induced the p53 pathway in NCM460 cells but not DLD-1 or SW480 cells. The mutated p53 function in the cancerous cell lines might have contributed to the observed

difference. NCM460, DLD-1, and SW480 cell lines experienced an increase in checkpoint kinase 1 (Chk-1), leading to cell cycle arrest. Not all cancerous cell lines are incapable of inducing the p53 pathway. For instance, cancerous A549 cells experienced an increase in the expression of p53 upon exposure to TiO_2 [61]. TiO_2 was found to induce double-strand breaks and a downregulation of cyclin B1 (a protein involved in mitosis) in A549 cells, leading to cell cycle arrest in the G_2/M phase [61]. CuO exposure causes the downregulation of various genes that allow cells to progress through the cycle at a couple of checkpoints in A549 cells [59]. Exposure of CuO downregulates proliferating cell nuclear antigen (PCNA, involved in proliferation), cell-division cycle protein (CDC2), and cyclin B1 (CCNB1, involved in G_2 to M transition) [59]. ZnO exposure causes DNA damage and the downregulation of cyclin B1 and cyclin-dependent kinase 1 (CDK1) in human immortal keratinocyte cells (HaCaT), causing G_2 arrest. PCNA was also downregulated [54]. Further studies are needed to demonstrate what genes cause cells to become arrested in the S or G_0/G_1 phase of the cell cycle. A systematic study looking at the gene responses after exposing a cell to different nanoparticles that lead to phase-specific changes in the cell cycle could provide evidence of how the characteristics of nanoparticles induce specific changes. It is possible for cells in cell cycle arrest to recover and continue proliferating upon the removal of nanoparticles. A549 cells whose proliferation is halted by CuO exposure could start proliferating again if cultured in a fresh medium. Reduction of stress can also allow cells to recover from cell cycle arrest. For instance, ZnO nanoparticle exposure induces G_2/M arrest in intestinal cell lines and the addition of antioxidant N-acetylcysteine can reverse cell cycle arrest by approximately 50–70% [69].

Table 2. Changes in cell cycle upon exposure to nanoparticles with a variety of characteristics in various cell lines.

Cell Line	Nanoparticle	Size (nm)	Specific Surface Area (m^2/g)	Zeta Potential (mV)	Shape	Effect on Cell Cycle	Reference
Human alveolar adenocarcinoma (A549)	TiO_2	>100	---	---	irregular	$\uparrow G_0/G_1$	[59]
A549	Fe_2O_3	39.2 *	---	---	spherical	No change	[50]
A549	CuO	50	---	−23.96 **	sphere	$\uparrow G_2/M$	[58,66]
A549	CuO	>50	---	---	irregular	$\uparrow G_2/M$	[59]
A549	NiO	50, 80 *, 450 **	61.16	−12; −22	---	$\downarrow G_0/G_1$ $\uparrow G_2/M$ $\uparrow$sub G_0	[56]
A549	ZnO	63.1 *	---	---	nearly spherical	$\uparrow G_2/M$	[50]
A459	TiO_2	23.28 ± 2.0 ** 106.7 ± 8.0 * 4-8	12-15	−10.16 ± 1.0 ** −13 ± 0.9 *	anatase	$\uparrow G_2/M$	[60]
A549	TiO_2	<5 65.3 **	200	−0.55 **	anatase	$\uparrow G_2/M$ $\downarrow G_0/G_1$	[51]
Human bronchial epithelial cells (BEAS-2B)	Fe_2O_3	39.2 *	---	---	spherical	No change	[50]
BEAS-2B	NiO	50	---	−12/−22	---	$\uparrow G_0/G_1$ $\downarrow G_2/M$ $\downarrow$S $\uparrow$Sub G_0	[56]
BEAS-2B	ZnO	63.1 *	---	---	nearly spherical	No change	[50]
Human immortal keratinocyte cells (HaCaT)	TiO_2	12 **	---	−11.9 ± 0.8 **	spherical	$\downarrow G_0/G_1$ $\uparrow$S	[57]
HaCaT	ZnO	<100 132.55 ± 0.45 **	15–25	−12.6 ± 0.95 **	rod-shaped	$\uparrow G_2/M$ $\downarrow$S	[53]
HaCaT	CuO	3–6 *	---	~37.5 *	---	$\uparrow G_2/M$ $\downarrow G_0/G_1$ $\downarrow$S	[61]

Table 2. Changes in cell cycle upon exposure to nanoparticles with a variety of characteristics in various cell lines (cont…).

Rat pheochromocytoma (PC12)	TiO_2	20	---	−12.5	anatase	↑G_2/M	[33]
Rat PC12	TiO_2	20	---	−23.2	rutile	↑G_2/M	[33]
Human neuroplastoma (SHSY5Y)	ZnO	100 243.7 * 273.4 **	15–20	−8.23 * −11.7 **	---	↓G_0/G_1 ↓G_2/M ↑S	[65]
Human mesenchymal stem cells (hMSFs)	Al_2O_3	20–100 205*	---	---	spherical	↓ G_0/G_1 ↓ G_2/M ↑Sub G_0	[62]
Human hMSFs	Fe_3O_4	50–75 119 * 210 **	---	---	spherical	↓ G_0/G_1 ↑Sub G_0	[52]
Human hepatoma (BEL-7402)	Fe_3O_4	10-30	---	14.4	---	↑G_0/G_1 ↓ S	[29]
Human epidermal carcinoma (A431)	ZnO	215.8 ± 0.1 * 30.9 ± 0.5 *	---	−25.3 ± 0.4 * −12.8 ± 0.6 **	---	↑S ↑G_2/M	[64]
Allium cepa root cells	ZnO	75–85	---	---	mostly cuboidal to hexagonal-octagonal, some rod	↓G_0/G_1 ↑G_2/M ↑Sub G_0	[63]
Mouse embryonic fibroblast (MEF)	CuO	3-6	---	~37.5	---	↑G_2/M ↓G_0/G_1 ↓S	[61]
Xenopus laevis (A6)	Poly-CuO	100 40–500 *	---	---	---	↑G_2/M ↓S	[67]
Xenopus laevis (A6)	CuO	6 ± 1 9-40 *	---	---	---	↑G_2/M	[67]

* Measured in water, ** Measured in cell culture medium, ↓ Decrease in cell number, ↑ Increase in cell number, --- Data not available.

5. CYTOTOXICITY IS A FUNCTION OF CELL KILLING AND SUPPRESSION OF PROLIFERATION

Numerous mechanisms may involve toxicity induced by exposure to nanoparticles. Altered signaling pathways perturb cellular homeostasis leading to cellular injuries. Nanotoxicity could lead to suppression of proliferation (via cell cycle arrest). When cells cannot overcome the stress and fix the damage, they are destined to death (apoptosis or necrosis). While the mechanisms that determine which cell cycle phase could become arrested are multiple, the consequential suppression of proliferation affects the cell number from one generation of cells to the next. Using the tritiated thymidine incorporation assay, we recently demonstrated that seven transition metal oxide nanoparticles can differentially suppress cell proliferation [70] (unpublished data). Assuming the doubling time of a cell line is 24 h and the rate of doubling time of cells is not altered, upon exposure to nanoparticles over a period of 24 h, the estimated number of cells in the second generation is expected to be as follows:

$$\text{Cell \# in Generation} = 2(\text{Proliferating cells}) + \text{non proliferating cells} - \text{dead cells}$$

Future studies should weigh the contribution of these two independent variables to the alteration in cell number.

6. CONCLUSIONS

Nanotoxicology emerged approximately at the turn of the century. Numerous studies have been conducted to better understand the impact nanomaterials have on environmental and human health and help us move toward making safer materials. In vitro studies are essential to identify biochemical and molecular mechanisms of cytotoxicity as the complexities of toxicokinetics and toxicodynamics typically observed in animal studies do not exist. In vitro studies provide insight to hazard identification which can lead to further studies on animal subjects. They are also the first step in identifying occupational risk assessment. Cumulative studies could potentially lead to a characterization model that allows workers to become aware of the potential risks of nanoparticle exposure. Preliminary data from in vitro experiments can potentially provide a precautionary risk management system in which workers are educated on the nanoparticles that have been shown to produce toxic and carcinogenic effects in in vitro experiments [28]. Properties of nanoparticles that contribute to cytotoxicity include, but are not limited to, surface, particle size, particle morphology, and dissolution of ions. As oxidative stress is elevated, and intracellular calcium homeostasis is perturbed due to exposure to nanoparticles, subsequent actions lead to cell injury and death, and deregulation of the cell cycle. The change in cell number is a function of cell killing and the suppression of proliferation. Deregulation of the cell cycle could result in cell death, non-proliferation, or recovery (upon removal of nanoparticles). Although the scientific community has made considerable strides in understanding nanotoxicity in the recent past, the future research needed to decipher nanotoxicity remain significant. For instance,

what are the properties of the nanoparticle that induce oxidative stress? How do nanoparticles interact, physically and chemically, with biomolecules such as nucleic acids, proteins, and lipids leading to alteration of gene expression? What is the basic scientific principle that dictates the shape-dependent cytotoxicity? Last but not least, quantification of cellular uptake of nanoparticles using single-particle ICP-MS may help with (1) the correlation of dose–effect and (2) the contribution of dissolved ions to cytotoxicity. As more information is gathered, it may be possible to apply the concept of quantitative structure and activity relationship (QSAR) to systematically delineate the cause–effect relationship. This could further improve the safety of the nanomaterial worker.

Conflicts of Interest: The authors declare no conflict of interest.

REFERENCES

1. Jones, B.J.; Vergne, M.J.; Bunk, D.M.; Locascio, L.E.; Hayes, M.A. Cleavage of Peptides and Proteins Using Light-Generated Radicals from Titanium Dioxide. *Anal. Chem.* **2007**, *79*, 1327–1332.

2. TIME. TIME's Best Inventions of 2008. Available online: http://content.time.com/time/specials/packages/article/0,28804,1852747_1854195_1854176,00.html (accessed 19 October 2017).

3. Earle, M.D. The Electrical Conductivity of Titanium Dioxide. *Phys. Rev.* **1942**, *61*, 56–62.

4. Hogan, J. Smog-busting paint soaks up noxious gases. *New Scientist*, 4 February 2004.

5. Phillips, L.G.; Barbano, D.M. The Influence of Fat Substitutes Based on Protein and Titanium Dioxide on the Sensory Properties of Lowfat Milks. *J. Dairy Sci.* **1997**, *80*, 2726–2731.

6. Fujishima, A. Discovery and applications of photocatalysis—Creating a comfortable future by making use of light energy. *Jpn. Nanonet Bull.* **2005**, *44*, 1–3.

7. Fujishmia, A.; Honda, K. Electrochemical Photolysis of Water at a Semiconductor Electrode. *Nature* **1972**, *238*, 37–38.

8. Vaidhyanathan, B.; Balaji, K.; Rao, K.J. Microwave-Assisted Solid-State Synthesis of Oxide Ion Conducting Stabilized Bismuth Vanadate Phases. *Chem. Mater.* **1998**, *10*, 3400–3404.

9. Greenwood, N.N.; Earnshaw, A. *Chemistry of the Elements*, 2nd ed.; Butterworth-Heinemann: Oxford, UK; Boston, MA, USA, 1997.

10. Page, E.M.; Wass, S.A. Vanadium:Inorganic and Coordination Chemistry. In *Encyclopedia of Inorganic Chemistry*; John Wiley & Sons: Hoboken, NJ, USA, 1994.

11. Adlam, G.H.J.; Price, L.S. *Higher School Certificate Inorganic Chemistry*; Anybook Ltd.: Lincoln, UK, 1945.

12. Greedon, J.E. Magnetic oxides. In *Encyclopedia of Inorganic Chemistry*; King, R.B., Ed.; John Wiley & Sons: Hoboken, NJ, USA, 1994.

13. Babes, L.; Denizot, B.; Tanguy, G.; Jacques Le Jeunne, J.; Jallet, P. Synthesis of Iron Oxide Nanoparticles Used as MRI Contrast Agents: A Parametric Study. *J. Colloid Interface Sci.* **1999**, *212*, 474–482.

14. Lee, S. *Encyclopedia of Chemical Processing*; CRC Press: Boca Raton, FL, USA, 2005.

15. Buxbaum, G.; Pfaff, G. *Industrial Inorganic Pigments*, 3rd ed.; Wiley: Hoboken, NJ, USA, 2005.

16. AZoNano. Copper Oxide (CuO) Nanoparticles—Properties, Applications. Available online: https://www.azonano.com/article.aspx?ArticleID=3395 (accessed on 21 October 2017).

17. Kenney, C.W.; Uchida, L.A. Use of Copper (II) Oxide as Source of Oxygen for Oxidation Reactions. Available online: http://www.freepatentsonline.com/4582613.html (accessed on 21 October 2017).

18. Saito, M. Antibacterial, Deodorizing, and UV Absorbing Materials Obtained with Zinc Oxide (ZnO) Coated Fabrics. *J. Ind. Text.* **1993**, *23*, 150–164.

19. Li, Q.; Chen, S.-L.; Jiang, W.-C. Durability of nano ZnO antibacterial cotton fabric to sweat. *J. Appl. Polym. Sci.* **2007**, *103*, 412–416.

20. Akhavan, O.; Ghaderi, E. Enhancement of antibacterial properties of Ag nanorods by electric field. *Sci. Technol. Adv. Mater.* **2009**, *10*, 015003.

21. AZoNano. Zinc Oxide (ZnO) Nanoparticles—Properties, Applications. Available online: https://www.azonano.com/article.aspx?ArticleID=3348 (accessed on 21 October 2017).

22. Li, Y.B.; Bando, Y.; Golberg, D. ZnO nanoneedles with tip surface perturbations: Excellent field emitters. *Appl. Phys. Lett.* **2004**, *84*, 3603–3605.

23. Kumar, S.A.; Chen, S.M. Nanostructured Zinc Oxide Particles in Chemically Modified Electrodes for Biosensor Applications. *Anal. Lett.* **2008**, *41*, 141–158.

24. Qin, Y.; Wang, X.; Lin Wang, Z. Editor's summary: Nanomaterial: Power dresser. *Nature* **2008**, *451*, 809–813.

25. Choi, C.H.; Alabi, C.A.; Webster, P.; Davis, M.E. Mechanism of active targeting in solid tumors with transferrin-containing gold nanoparticles. *Proc. Natl. Acad. Sci. USA* **2010**, *107*, 1235–1240.

26. Korin, N.; Kanapathipillai, M.; Ingber, D.E. Sheer-responsive platemet mimetics for targeted drug delivery. *Isr. J. Chem.* **2012**, *53*, 610–615.

27. Highsmith, J. Nanoparticles in Biotechnology, Drug Development and Drug Delivery. In *Global Markets: A BCC Research Report*; BCC Research: Wellesley, MA, USA, 2014.

28. Leso, V.; Fontana, L.; Mauriello, M. C.; Iavicoli, I. Occupational risk assessment of engineered nanomaterials challenges and opportunities. *Curr. Nanosci.* **2017**, *13*, 55–78.

29. Jiang, J.; Oberdorster, G.; Elder, A.; Gelein, R.; Mercer, P.; Biswas, P. Does Nanoparticle Activity Depend upon Size and Crystal Phase? *Nanotoxicology* **2008**, *2*, 33–42.

30. Kai, W.; Xiaojun, X.; Ximing, P.; Zhenqing, H.; Qiqing, Z. Cytotoxic effects and the mechanism of three types of magnetic nanoparticles on human hepatoma BEL-7402 cells. *Nanoscale Res. Lett.* **2011**, *6*, 480.

31. Baek, M.; Kim, M.K.; Cho, H.J.; Lee, J.A.; Yu, J.; Chung, H.E.; Choi, S.J. Factors influencing the cytotoxicity of zinc oxide nanoparticles: Particle size and surface charge. *J. Phys. Conf. Ser.* **2011**, *304*, 012044.

32. Huang, Y.W.; Lee, H.J.; Tolliver, L.M.; Aronstam, R.S. Delivery of nucleic acids and nanomaterials by cell-penetrating peptides: Opportunities and challenges. *BioMed Res. Int.* **2015**, *2015*, 834079.

33. Chusuei, C.C.; Wu, C.H.; Mallavarapu, S.; Hou, F.Y.; Hsu, C.M.; Winiarz, J.G.; Aronstam, R.S.; Huang, Y.W. Cytotoxicity in the age of nano: The role of fourth period transition metal oxide nanoparticle physicochemical properties. *Chem.-Biol. Interact.* **2013**, *206*, 319–326.

34. Wu, J.; Sun, J.; Xue, Y. Involvement of JNK and P53 activation in G2/M cell cycle arrest and apoptosis induced by titanium dioxide nanoparticles in neuron cells. *Toxicol. Lett.* **2010**, *199*, 269–276.

35. Lee, J.H.; Ju, J.E.; Kim, B.I.; Pak, P.J.; Choi, E.K.; Lee, H.S.; Chung, N. Rod-shaped iron oxide nanoparticles are more toxic than sphere-shaped nanoparticles to murine macrophage cells. *Environ. Toxicol. Chem.* **2014**, *33*, 2759–2766.

36. Forest, V.; Leclerc, L.; Hochepie, J.F.; Trouvé, A.; Sarry, G.; Pourchez, J. Impact of Cerium Oxide Nanoparticles Shape on their In Vitro Cellular Toxicity. *Toxicol. In Vitro* **2017**, *38*, 136–141.

37. Delorme, M.P.; Muro, Y.; Arai, T.; Banas, D.A.; Frame, S.R.; Reed, K.L.; Warheit, D.B. Ninety-day inhalation toxicity study with a vapor grown carbon nanofiber in rats. *Toxicol. Sci.* **2012**, *128*, 449–460.

38. Guttenberg, M.; Bezerra, L.; Neu-Baker, N.M.; del Pilar Sosa Idelchik, M.; Elder, A.; Oberdorster, G.; Brenner, S.A. Biodistribution of inhaled metal oxide nanoparticles mimicking occupational exposure: A preliminary investigation using enhanced darkfield microscopy. *J. Biophotonics* **2016**, *9*, 987–993.

39. Oberdorster, G. Safety assessment for nanotechnology and nanomedicine: Concepts of nanotoxicology. *J. Intern. Med.* **2010**, *267*, 89–105.

40. Warheit, D.B.; Webb, T.R.; Colvin, V.L.; Reed, K.L.; Sayes, C.M. Pulmonary bioassay studies with nanoscale and fine-quartz particles in rats: Toxicity is not dependent upon particle size but on surface characteristics. *Toxicol. Sci.* **2007**, *95*, 270–280.

41. Stone, V.; Miller, M.R.; Clift, M.J.D.; Elder, A.; Mills, N.L.; Møller, P.; Schins, R.P.F.; Vogel, U.; Kreyling, W.G.; Alstrup Jensen, K.; et al. Nanomaterials Versus Ambient Ultrafine Particles: An Opportunity to Exchange Toxicology Knowledge. *Environ. Health Perspect.* **2017**, *125*, 106002.

42. Nel, A.; Xia, T.; Madler, L.; Li, N. Toxic Potential of Materials at the Nanolevel. *Science* **2006**, *311*, 622–627.

43. Xia, T.; Kovochich, M.; Brant, J.; Hotze, M.; Sempf, J.; Oberley, T.; Sioutas, C.; Yeh, J.I.; Wiesner, M.R.; Nel, A.E. Comparison of the Abilities of Ambient and Manufactured Nanoparticles To Induce Cellular Toxicity According to an Oxidative Stress Paradigm. *Nano Lett.* **2006**, *6*, 1794–1807.

44. Lin, W.; Huang, Y.W.; Zhou, X.D.; Ma, Y. In vitro toxicity of silica nanoparticles in human lung cancer cells. *Toxicol. Appl. Pharmacol.* **2006**, *217*, 252–259.

45. Lin, W.; Huang, Y.W.; Zhou, X.D.; Ma, Y. Toxicity of cerium oxide nanoparticles in human lung cancer cells. *Int. J. Toxicol.* **2006**, *25*, 451–457.

46. Lin, W.; Xu, Y.; Huang, C.-C.; Ma, Y.; Shannon, K.B.; Chen, D.-R.; Huang, Y.-W. Toxicity of nano- and micro-sized ZnO particles in human lung epithelial cells. *J. Nanopart. Res.* **2009**, *11*, 25–39.

47. Huang, C.C.; Aronstam, R.S.; Chen, D.R.; Huang, Y.W. Oxidative stress, calcium homeostasis, and altered gene expression in human lung epithelial cells exposed to ZnO nanoparticles. *Toxicol. In Vitro* **2010**, *24*, 45–55.

48. Lin, W.; Stayton, I.; Huang, Y.-W.; Zhou, X.-D. Cytotoxicity and cell membrane depolarization induced by aluminum oxide nanoparticles in human lung epithelial cells A549. *Toxicol. Environ. Chem.* **2008**, *90*, 983–996.

49. Wang, H.J.; Growcock, A.C.; Tang, T.H.; O'Hara, J.; Huang, Y.W.; Aronstam, R.S. Zinc oxide nanoparticle disruption of store-operated calcium entry in a muscarinic receptor signaling pathway. *Toxicol. In Vitro* **2010**, *24*, 1953–1961.

50. Tang, T.H.; Chang, C.T.; Wang, H.J.; Erickson, J.D.; Reichard, R.A.; Martin, A.G.; Shannon, E.K.; Martin, A.L.; Huang, Y.W.; Aronstam, R.S. Oxidative stress disruption of receptor-mediated calcium signaling mechanisms. *J. Biomed. Sci.* **2013**, *20*, 48.

51. Lai, X.; Wei, Y.; Zhao, H.; Chen, S.; Bu, X.; Lu, F.; Qu, D.; Yao, L.; Zheng, J.; Zhang, J. The effect of Fe_2O_3 and ZnO nanoparticles on cytotoxicity and glucose metabolism in lung epithelial cells. *J. Appl. Toxicol.* **2015**, *35*, 651–664.

52. Wang, Y.; Cui, H.; Zhou, J.; Li, F.; Wang, J.; Chen, M.; Liu, Q. Cytotoxicity, DNA damage, and apoptosis induced by titanium dioxide nanoparticles in human non-small cell lung cancer A549 cells. *Environ. Sci. Pollut. Res. Int.* **2015**, *22*, 5519–5530.

53. Periasamy, V.S.; Athinarayanan, J.; Alhazmi, M.; Alatiah, K.A.; Alshatwi, A.A. Fe_3O_4 nanoparticle redox system modulation via cell-cycle progression and gene expression in human mesenchymal stem cells. *Environ. Toxicol.* **2016**, *31*, 901–912.

54. Gao, F.; Ma, N.; Zhou, H.; Wang, Q.; Zhang, H.; Wang, P.; Hou, H.; Wen, H.; Li, L. Zinc oxide nanoparticles-induced epigenetic change and G2/M arrest are associated with apoptosis in human epidermal keratinocytes. *Int. J. Nanomed.* **2016**, *11*, 3859–3874.

55. Saptarshi, S.R.; Duschl, A.; Lopata, A.L. Interaction of nanoparticles with proteins: Relation to bio-reactivity of the nanoparticle. *J. Nanobiotechnol.* **2013**, *11*, 26.

56. Chang, Y.-N.; Zhang, M.; Xia, L.; Zhang, J.; Xing, G. The Toxic Effects and Mechanisms of CuO and ZnO Nanoparticles. *Materials* **2012**, *5*, 2850–2871.

57. Capasso, L.; Camatini, M.; Gualtieri, M. Nickel oxide nanoparticles induce inflammation and genotoxic effect in lung epithelial cells. *Toxicol. Lett.* **2014**, *226*, 28–34.

58. Gao, X.; Wang, Y.; Peng, S.; Yue, B.; Fan, C.; Chen, W.; Li, X. Comparative toxicities of bismuth oxybromide and titanium dioxide exposure on human skin keratinocyte cells. *Chemosphere* **2015**, *135*, 83–93.

59. Hanagata, N.; Zhuang, F.; Connolly, S.; Li, J.; Ogawa, N.; Xu, M. Molecular Responses of Human Lung EpithelialCellstotheToxicityofCopper Oxide Nanoparticles Inferred from Whole Genome Expression Analysis. *ACS Nano* **2011**, *5*, 9326–9338.

60. Moschini, E.; Gualtieri, G.; Gallinotti, D.; Pezzolato, E.; Fascio, U.; Camatini, M.; Mantecca, P. Metal oxide nanoparticles induce cytotoxic effects on human lung epithelial cells A549. *Chem. Eng. Trans.* **2010**, *22*, 29–34.

61. Kansara, K.; Patel, P.; Shah, D.; Shukla, R.K.; Singh, S.; Kumar, A.; Dhawan, A. TiO_2 nanoparticles induce DNA double strand breaks and cell cycle arrest in human alveolar cells. *Environ. Mol. Mutagen.* **2015**, *56*, 204–217.

62. Luo, C.; Li, Y.; Yang, L.; Zheng, Y.; Long, J.; Jia, J.; Xiao, S.; Liu, J. Activation of Erk and p53 regulates copper oxide nanoparticle-induced cytotoxicity in keratinocytes and fibroblasts. *Int. J. Nanomed.* **2014**, *9*, 4763–4772.

63. Periasamy, V.S.; Athinarayanan, J.; Alshatwi, A.A. Aluminum oxide nanoparticles alter cell cycle progression through *CCND1* and *EGR1* gene expression in human mesenchymal stem cells. *Biotechnol. Appl. Biochem.* **2016**, *63*, 320–327.

64. Ghosh, M.; Jana, A.; Sinha, S.; Jothiramajayam, M.; Nag, A.; Chakraborty, A.; Mukherjee, A.; Mukherjee, A. Effects of ZnO nanoparticles in plants: Cytotoxicity, genotoxicity, deregulation of antioxidant defenses, and cell-cycle arrest. *Mutat. Res. Genet. Toxicol. Environ. Mutagen.* **2016**, *807*, 25–32.

65. Patel, P.; Kansara, K.; Senapati, V.A.; Shanker, R.; Dhawan, A.; Kumar, A. Cell cycle dependent cellular uptake of zinc oxide nanoparticles in human epidermal cells. *Mutagenesis* **2016**, *31*, 481–490.

66. Valdiglesias, V.; Costa, C.; Kilic, G.; Costa, S.; Pasaro, E.; Laffon, B.; Teixeira, J.P. Neuronal cytotoxicity and genotoxicity induced by zinc oxide nanoparticles. *Environ. Int.* **2013**, *55*, 92–100.

67. Xu, M.; Fujita, D.; Kajiwara, S.; Minowa, T.; Li, X.; Takemura, T.; Iwai, H.; Hanagata, N. Contribution of physicochemical characteristics of nano-oxides to cytotoxicity. *Biomaterials* **2010**, *31*, 8022–8031.

68. Thit, A.; Selck, H.; Bjerregaard, H.F. Toxicity of CuO nanoparticles and Cu ions to tight epithelial cells from *Xenopus laevis* (A6): Effects on proliferation, cell cycle progression and cell death. *Toxicol. In Vitro* **2013**, *27*, 1596–1601.

69. Setyawati, M.I.; Tay, C.Y.; Leong, D.T. Mechanistic Investigation of the Biological Effects of SiO_2, TiO_2, and ZnO Nanoparticles on Intestinal Cells. *Small* **2015**, *11*, 3458–3468.

70. Tolliver, L.; Cambre, M.; Hou, F. Y.; Lee, H. J.; Aronstam, R.; Huang, Y. W., Nanotoxicity of Transition Metal Oxides is a Function of Cell Killing and Suppression of Cell Proliferation. *Toxicology In Vitro,* **In prep**.

II. DIFFERENTIAL CYTOTOXICITY OF NiO AND $Ni(OH)_2$ NANOPARTICLES IS MEDIATED BY OXIDATIVE STRESS-INDUCED CELL DEATH AND SUPPRESSION OF CELL PROLIFERATION

ABSTRACT

The use of nanomaterial-based products continues to grow with advancing technology. Understanding the potential toxicity of nanoparticles (NPs) is important to ensure that these new products do not impose harmful effects to human and environmental health. In this project, we evaluated the differential cytotoxicity between nickel oxide (NiO) and nickel hydroxide $Ni(OH)_2$ in human bronchoalveolar carcinoma (A549) and human hepatocellular carcinoma (HepG2) cell lines. The sulforhodamine B assay was used measure cellular viability after 10, 25, 50, 75, and 100 μg/mL of NiO and $Ni(OH)_2$ NPs for 24h and 48h. Cellular viability assays revealed cell line-specific cytotoxicity in which nickel NPs were toxic to A549 cells but relatively nontoxic to HepG2 cells. Time-, concentration-, and particle-specific viability was observed in A549 cells. NP-induced oxidative stress triggered subsequent dissipation of mitochondrial membrane potential and induction of caspase-3 enzyme activity. The subsequent apoptotic events lead to reduction in cell number, though the contribution of necrosis to cell viability is unknown. In addition to cell death, suppression of cell proliferation contributes to play an essential role in regulating cell number. Elevated OS had a strong correlation with viability. Collectively, the observed cell viability is a function of cell death and suppression of proliferation.

1. INTRODUCTION

Nanomaterials have become increasingly popular in the production of a wide range of products including cosmetics [1], pharmaceuticals [2], medical research [3], semiconductor fabrication [4], food [5], electronic manufacturing [6], and many other products. Nanomaterial-based products are estimated to reach $79.8 billion in the global market by the year 2019 [7]. The increase in the use of nanoparticles (NPs) may increase the risk of human exposure via air, water, and food. Workers in various industries are at higher risk of exposure to NPs via inhalation [8]. While some NPs are relatively harmless, others have been shown to produce moderate to severe toxic effects In vitro studies have demonstrated that NPs can become internalized within the cells where they can cause damage [9-13]. Such damages include increase of reactive oxidative stress, mitochondrial dysfunction, severe damage of DNA, cell cycle arrest, induction of apoptosis and increase in necrosis [14]. These changes within the cell affect overall cell viability.

Toxicity depends on physicochemical properties of NPs [15]. For example, morphology of TiO_2 NPs affects cytotoxicity. The amorphous form of TiO_2 generated the most reactive oxygen species (ROS) followed by anatase and then rutile [16]. Rod-shaped CeO_2 produced toxic responses in RAW 264.7 cells while the octahedron and cubic elicited little responses [17]. Surface charge may also influence toxicity, with positively charged ZnO producing a higher degree of toxicity than negatively charged particles in A549 cells [18]. Three iron NPs (Fe_3O_4, OA- Fe_3O_4, and C-Fe) with different positive charges were found to produce toxic responses in A549 cells that

positively correlated with the charge [19]. Dissolution rate, relative available binding sites on particle surface, and particle surface charge of various transition metal oxides correlated with toxicity in A549 cells [20]. It is important to note that the mechanisms of toxicity of NPs are not always, but can be, cell line-dependent [9, 21]. For instance, NiO NPs arrest BEAS-2B cells in the G_1 phase while arrest of A549 cells occurs in the G_2/M phase [21]. Furthermore, NiO NPs induce a higher rate of apoptosis in BEAS-2B cells than A549 cells. Additionally, ZnO exposure induces cell cycle alterations in A549 cells but not BEAS-2B cells [9].

Nickle NPs may impose risk on human health as they are widely used in various industries. NiO NPs are used in coloring agents for enamels, in nanowires, in automotive rear-view mirrors, and more products [22]. $Ni(OH)_2$ NPs are used in rechargeable battery electrodes, nickel cadmium batteries, and nickel metal hydride batteries [23]. Toxic responses upon exposure to NiO and $Ni(OH)_2$ NPs have been characterized in both in vivo and in vitro settings. Exposure to NiO or $Ni(OH)_2$ NPs induces inflammation in the lungs of rats [24, 25]. NiO was found to induce ROS and lipid peroxidation in A549 cells [26]. Exposure of NiO NPs induces oxidative stress, apoptosis, reduction in viability in breast cancer cell line MCF-7 and the human airway epithelial cell line HEp-2 [27]. Exposure to particulate and soluble nickel compounds led to differential toxicity in AS52 cells [28].

There are no studies comparing the difference in cellular toxicity upon exposure of NiO and $Ni(OH)_2$ NPs in A549 cells. Further, there have been no studies on the role of suppression of cell proliferation induced by NPs. Our preliminary data suggest that $Ni(OH)_2$ NPs decrease viability more significantly than NiO NPs. We thus

hypothesize that 1) cytotoxicity of NiO and $Ni(OH)_2$ NPs is cell line-, particle-, time-, and dose-dependent, 2) cytotoxicity is mediated by oxidative stress and subsequent cellular events including modulation of mitochondrial membrane potential and caspase-3 enzyme activity, and 3) exposure to NiO and $Ni(OH)_2$ NPs alters cell cycle leading to suppression of cell proliferation. Our specific aims are to: 1) demonstrate that cytotoxicity is cell line-, particle-, time- and dose- dependent, 2) measure the differences in various biochemical responses upon NiO or $Ni(OH)_2$ exposure, and 3) investigate that cell viability is a function of cell killing and inhibition of cell proliferation. To achieve our goals, we measured cell viability in a liver cell line (HepG2) and a lung cell line (A549) upon NiO or $Ni(OH)_2$ exposure. We then delineated the mechanism of action of toxicity in the context of oxidative stress-mediated cellular injuries, including mitochondrial membrane potential, caspase-3 activity, apoptosis, cell cycle, and proliferation.

2. MATERIALS AND METHODS

2.1. SOURCES OF MATERIALS

NiO was purchased from Nanostructured and Amorphous Materials (Los Alamos, New Mexico, USA). $Ni(OH)_2$ was purchased from US Research Nanomaterials (Houston, Texas, USA). Human bronchoalveolar carcinoma-derived (A549) cells and human liver hepatocellular carcinoma (HepG2) cells were acquired from American Tissue Culture Collection (Manassas, VA, USA). H_2DCFDA and propidium iodide were obtained from Fisher Scientific (St. Peters, MO, USA). The JC-1 Mitochondrial

Membrane Potential Detection Kit and sulforhodimine B were purchased from Biotium (Freemont, CA, USA). Ac-DEVD-pNA was obtained from Anaspec (Fremont, CA, USA). Annexin V-FITC and 7-aminoactinomycin D (7-AAD) were acquired from BD Biosciences (San Jose, CA, USA). Tritiated thymidine was purchased from Perkin-Elmer (Downers Grove, IL, USA). Other chemicals used for experiments were of the highest purity that they could be obtained.

2.2. STORAGE AND CHARACTERIZATION OF NANOPARTICLES

NPs were stored in an amber desiccator under a pure nitrogen atmosphere to protect them from moisture, oxidation, and UV damage. The instrumentation and protocols used to characterize NPs followed our previous publications [29]. Specific surface area (SSA) and shape of NPs in non-aqueous conditions were measured by Brunauer-Emmett-Teller (BET) and X-Ray Diffraction (XRD), respectively. Size, shape, surface charge, and relative available surface binding sites of NPs in aqueous conditions were measured by transition electron microscopy (TEM) and point of zero charge (PZC).

2.3. CELL CULTURE AND NANOPARTICLE TREATMENT

2.3.1. Cell Line Maintenance. A549 cells were maintained in Hams F-12 modified medium supplemented with 10% fetal clone serum and 1% penicillin/streptomycin. HepG2 cells were maintained in Eagle's minimum essential medium supplemented with 10% fetal clone serum and 1% penicillin/streptomycin. Both cell lines were grown in 10 cm tissue culture dishes at 37°C in a 5% CO_2 humidified

incubator. All cells were grown to a confluence of ca. 70-80% before the next passage. Appropriate numbers of cells were seeded for various experiments (Appendix A1).

2.3.2. Exposure of Cells to Nanoparticles. NPs were dispersed evenly in cell culture medium before cells exposure in the following way. The NPs were weighed using an analytical balance. One milliliter of medium was added to create a final concentration of 1 mg NP per 1 mL medium. The samples were then sealed with parafilm and sonicated for 3 min to break up aggregates. The suspension was vortexed to achieve a homogenous mixture before adding to cells. Experiments performed using a 24 well plate were performed as a triplicate, and the average of each group was taken for each individual experiment.

2.4. CELL VIABILITY

Cell viability was measured using the sulforhodamine B assay (SRB). Upon termination of experiments, cell medium was discarded from the cells. The cells were fixed with cold 10% trichloroacetic acid (TCA) for 1h at 4^{o}C. The cells were then washed three times with distilled water and then allowed to dry completely. Cells were incubated with 0.5 mL SRB (0.2% in 1% acetic acid) for 30 min at room temperature. The cells were then washed with 1 mL of 1% acetic acid for 20 min on a rocker three times to eliminate excess dye. A Q-tip was used to remove excess solutions stuck to the sides of the wells. Acetic acid was removed followed by addition of 400 µL of cold 10 mM Tris hydrochloride solution to each well for 20 min. Aliquots of 250 µL each were transferred onto a 96-well plate. Absorbance was measured at 510 nm using a microplate reader (FLOURstar, BMG Labtechnologies, Durham, NC, USA). Cell viability of

treatment groups were calculated based on the percent absorbance relative to the control group.

2.5. REACTIVE OXIDATIVE SPECIES

Reactive oxidative species was measured with 2',7'-dichlorodihydrofluorescein diacetate (H_2DCFDA). Upon entrance of the cell, H_2DCFDA is deacetylated by esterases into a non-fluorescent compound. When H_2DCFDA is oxidized by reactive oxidative species, it is converted to the highly fluorescent compound 2',7'-dichlorofluorescein (DCF) that can be detected by fluorescence spectroscopy. Cells were exposed to a serious of concentrations of NPs (0, 10, 25, 50, 75, or 100 µg/mL) for 24h or 48h. For positive control, cells were incubated with 400 µM tert-butyl hydroperoxide (t-BHP) at 37°C for 1h before termination of the experiment. Upon termination of the dosing period the media was removed from the cells followed by a wash with PBS once. Eighty microliters of H_2DCFDA was added to each well for 1h. Cells were then washed with PBS three times followed by addition of 100 µL of PBS. Fluorescence was measured using a microplate reader (FLOURstar, BMG Labtechnologies, Durham, NC, USA) with excitation at 485 and emission at 510. The florescence intensity of cells in experimental plates will be divided by the fluorescence intensity in control cells to determine the percent increase in ROS.

2.6. MITOCHONDRIAL MEMBRANE POTENTIAL

Mitochondrial membrane potential was determined with microscopy using the JC-1 Mitochondrial Membrane Potential (MMP) Detection Kit. JC-1 in the cytosol exist as

green fluorescing monomers. Healthy mitochondria have a high negative potential that result in a high influx of cationic JC-1, increasing the JC-1 concentration by as high as 1000x. High concentrations of JC-1 form aggregates that fluoresce red. Unhealthy mitochondria have a lower negative potential and will therefore intake less JC-1. The JC-1 will remain in the cytosol as green fluorescing monomers.

Cells were exposed to a serious of concentrations of nanoparticles (0, 10, or 100 µg/mL) for 12h or 24h. Upon termination of experiments, the plates were incubated with JC-1 working solution at 37° C for 15 minutes. Each plate was then washed with 1 mL of PBS followed by addition of 1 mL of PBS before fluorescence detection under a fluorescence microscope. Rhodamine was observed with a Texas Red filter (ex/em 590/610 nm) while fluorescein with a FITC filter (ex/em 490/520 nm).

2.7. CASPASE-3 ACTIVITY

Caspase-3 enzymatic activity was measured using Ac-DEVD-pNA as a substrate. Cells were exposed to a serious of concentrations of NPs (0, 10, 25, 50, 75, or 100 µg/mL) for 24h or 48h. Upon termination of experiments, cells were washed with 0.5 mL of PBS. Lysis buffer (50mM Tris-HCl, 1.5 mL of 5 M NaCl, 0.25 g sodium deoxycholate, 1 mM EDTA, 0.5 mL Triton-100, 50 mL DI water) was added. Cells were scratched off the bottom, then resuspend in the lysis buffer and incubated in 4°C for 10 min. Samples were centrifuged at 15,000 g for 20 min at 4°C. Reaction buffer (20% glycerol, 0.5 mM EDTA, 5 mM dithiothreitol, 100 mM HEPES, pH 7.5) was added to cell lysate that contain 20 µg of cell protein in each well to make a total volume 198 µL per well. Then, 2 µl chromogenic Ac-DEVD-pNA substrate was added to each well.

Samples were incubated at 37° for 6h. Absorbance of enzyme-catalyzed release of p-nitroanilide is measured at 405 nm with a microplate.

2.8. CELL CYCLE

Alteration of cell cycle due to exposure NPs was measured with flow cytometry using propidium iodide (PI). Cells were exposed to a series of concentrations of NPs (0, 10, 25, 50, 75, or 100 µg/mL) for 24h or 48h. Upon termination of experiments, the cells were washed with PBS, harvested using trypsin, and centrifuged. The cell pellet was then re-suspended in 1 mL of PBS followed by the addition of 3 mL of cold absolute methanol to fix the cells. The cells were placed in the refrigerator for at least 24h to allow complete fixation. After fixation, the cells were centrifuged and then washed twice with 1x PBS (centrifuging in between each wash). The cells were then suspended in a PI staining solution (PI and ribonuclease A in 1x PBS) for 15 min in the dark. One mL of PBS was added to each sample before centrifuging. The supernatant was removed, and cells were resuspended in 250 µL PBS. The stained samples were then plated into a 96 well plate and analyzed with Cell Lab Quanta SC MPL flow cytometer. FCS Express 6 software was used to determine changes in cell cycle phase. The total number of cells in each phase of the cell cycle (G_0/G_1, S and G_2/M) was totaled and the percentage in each phase was calculated.

2.9. APOPTOSIS

Apoptosis was measured with flow cytometry using annexin V-FITC and 7-aminoactinomycin D (7-AAD). Cells were exposed to a series of concentrations of NPs

(0, 10, 25, 50, 75, or 100 µg/mL) for 24h or 48h. Upon termination of experiments, cells were washed with PBS, harvested with trypsin, and centrifuged. The supernatant was then discarded, and 1 mL of ice cold PBS was added to resuspend the pellet followed by centrifugation. After centrifugation, the supernatant was removed. The cells were resuspended in 100 µL of 1x concentrated annexin V binding buffer, 5 µL of annexin V-FITC and 5 µL of 7-AAD. The cells were incubated for 15 min in the dark. Another 200 µL of Annexin V binding buffer was then added to each tube and 150 µL of this cell/dye/binding buffer mixture was transferred to a 96 well microplate for flow cytometry analysis. Early and late apoptotic cells were added to determine the total percentage of apoptotic cells.

2.10. PROLIFERATION

Proliferation was determined with the tritiated thymidine (^{3}H-thymidine) incorporation assay. Cells were exposed to a series of concentrations of NPs (0, 10, 25, 50, 75, or 100 µg/mL) and ^{3}H-thymidine simultaneously for 24h or 48h. Upon termination of the experiment, cells were washed twice with ice cold 1x PBS. The cells were then fixed in 0.5 mL ice cold 10% TCA for 5 min on ice. TCA fixation was repeated once. Cells were brought to room temperature and lysed using a room-temperature 1 M NaOH solution for 5 min. The solution was neutralized by adding an equal amount of 1 M HCl. The lysed cell solution was thoroughly mixed by pipetting up and down and then transferred to scintillation vials with Econo-Safe scintillation counting fluid (Research Products International, Mt Prospect, IL, USA). These vials were then subject to scintillation counting using a Beckman liquid scintillation counter LS6500

(Beckman-Coulter, Fullerton, CA, USA). The total count of radioactivity was divided by the radioactivity from the control cells to determine the percentage of proliferating cells compared to unexposed cells.

2.11. STATISTICAL ANALYSIS AND FIGURES

Three to five independent experiments were conducted. Each individual experiment was run as a triplicate. Statistical analysis was performed in Minitab 18. Data sets are presented as means ± standard deviation, with the number of individual experiments defined as N. A one-way t-test was used to compare experimental groups to the control groups (μ>control or μ<control depending on the experimental hypothesis). One-way analysis of variance (ANOVA) with Tukey's post hoc pairwise comparison was used to determine significant differences among each treatment group. One-way ANOVA with Dunnett post hoc pairwise comparison was used to determine significant differences against the control group. Significance was set at $p<0.05$. All figures were produced using GraphPad Prism 7.

3. RESULTS

3.1. PHYSIOCOCHEMICAL PROPERTIES OF NIO AND $Ni(OH)_2$

The approximate physical sizes (APS) of NiO and $Ni(OH)_2$ were 16 ± 4 nm and 15 ± 5 nm, respectively (Table 1, Fig. 1). The specific surface area (SSA) of NiO was 73.5 m^2/g and the SSA of $Ni(OH)_2$ was 103.2 m^2/g (Table 1). The morphology

Table 1. Physical characteristics of NiO and $Ni(OH)_2$ NPs

	NiO	$Ni(OH)_2$
APS* (nm)	16.± 4.8	15. ± 4.9
SSA** (m^2/g)	73.5	103.2
Shape	Cubic	Hexagonal/rod

*APS denotes approximate physical size; length of the cubic NiO and length of the rod of $Ni(OH)_2$

**SSA denotes specific surface area

determined by X-ray Diffraction (XRD) analysis was cubic (NiO) or a hexagonal/rod shape ($Ni(OH)_2$) (Fig. 1). The PZC was 8.7 for NiO and 7.9 for $Ni(OH)_2$ (Fig. 2).

3.2. CELL VIABILITY

Two nickel NPs (NiO and $Ni(OH)_2$) were chosen for comparative toxicity in the context of cell viability, oxidative stress-induced cellular injuries, and suppression of cell proliferation. Results from cell viability of A549 and HepG2 revealed cell-line dependent cytotoxicity (Fig. 3A). NiO and $Ni(OH)_2$ did not produce as prominent cytotoxic effects in HepG2 cells as in A549 cells. There was no significant change in viability upon exposure to NiO for 24h or 48h or to $Ni(OH)_2$ for 24h in HepG2 cells ($N=3$, $p<0.05$). HepG2 exposure to $Ni(OH)_2$ at 75 and 100 µg/mL for 48h resulted in a significant decrease in viability to 71.2% and 72.6%, respectively. On the other hand, exposure to NiO or $Ni(OH)_2$ caused a significant reduction of toxicity in all experimental groups in A549 cells, which was not observed in HepG2 cells. At 24h, the lowest tested concentration (10 µg/mL) reduced viability to 84.3% and 81.3% when A549 cells were exposed to NiO or $Ni(OH)_2$, respectively (N-3, $p<0.05$) (Fig. 3B). These percentages

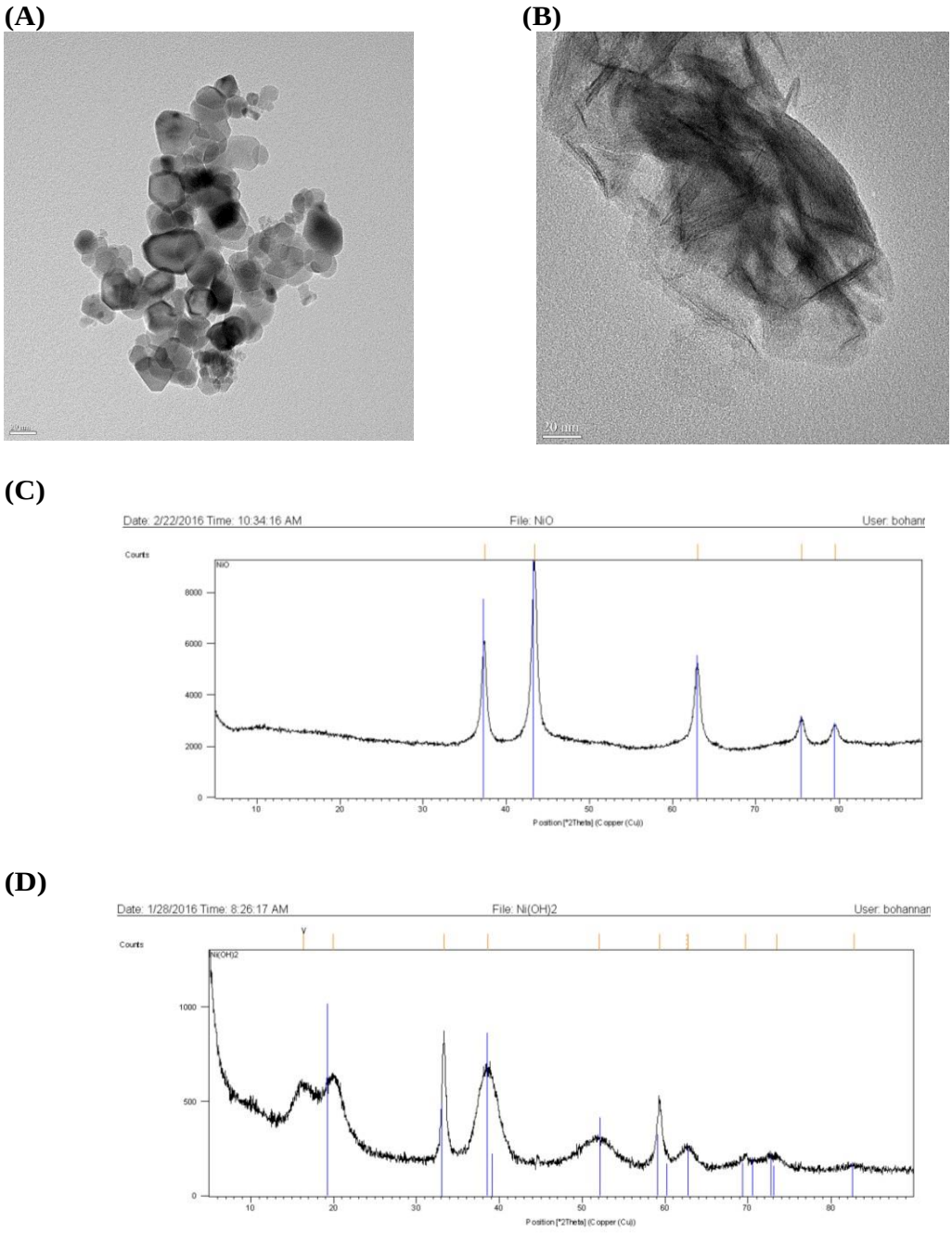

Figure 1. Morphology and crystalline structure. Morphology of NiO (A) and $Ni(OH)_2$ (B) NPs from transmission electron microscopy. Crystalline structure of NiO (C) and $Ni(OH)_2$ (D) NPs from XRD analysis. NiO has a cubic shape. $Ni(OH)_2$ possesses a long rod shape with a hexagonal top and bottom.

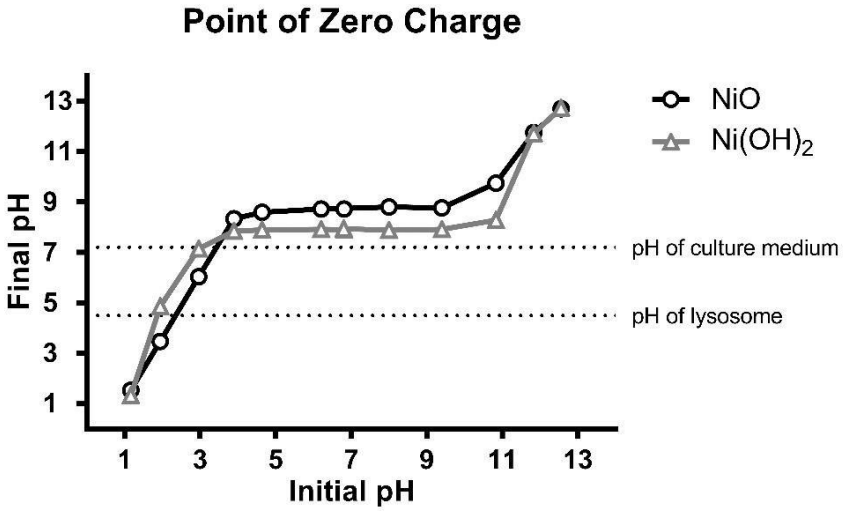

Figure 2. Point of zero charge (PZC) analysis of NiO and $Ni(OH)_2$. Results indicate that the PZCs of NiO and $Ni(OH)_2$ are 8.7 and 7.9.

were further reduced at 48h. At 48h, the highest tested concentration (100 µg/mL), reduced viability to 27.0% and 11.1% when A549 cells were exposed to NiO or $Ni(OH)_2$, respectively (N=3, $p<0.05$) (Fig. 3C). Viability of A549 cells was NP-, time-, and concentration- specific (Fig. 3B-D). A NP-specific viability was observed at both 24h and 48h. $Ni(OH)_2$ is more toxic than NiO at 25 µg/mL and above at 24h (N=3, $p<0.05$). At 100 µg/mL, $Ni(OH)_2$ reduced viability to 57.8% while NiO reduced viability to 39.2% (Fig. 3B). $Ni(OH)_2$ µg/mL is more toxic than NiO at 50 µg/mL and above at 48h (N=3, $p<0.05$). At 50 µg/mL, viability was reduced to 45.4% upon NiO exposure and to 32.9% upon $Ni(OH)_2$ exposure (Fig. 3C). Time-specific effects were manifested in an exposure duration of 48h. Both NiO and $Ni(OH)_2$ were more toxic at 48h than at 24h at all tested concentrations (N=3, $p<0.05$). Exposure to NiO reduced viability to 57.8% (24h) and 27.0% (48h) at 100 µg/mL. $Ni(OH)_2$ exposure reduced viability to 39.1%

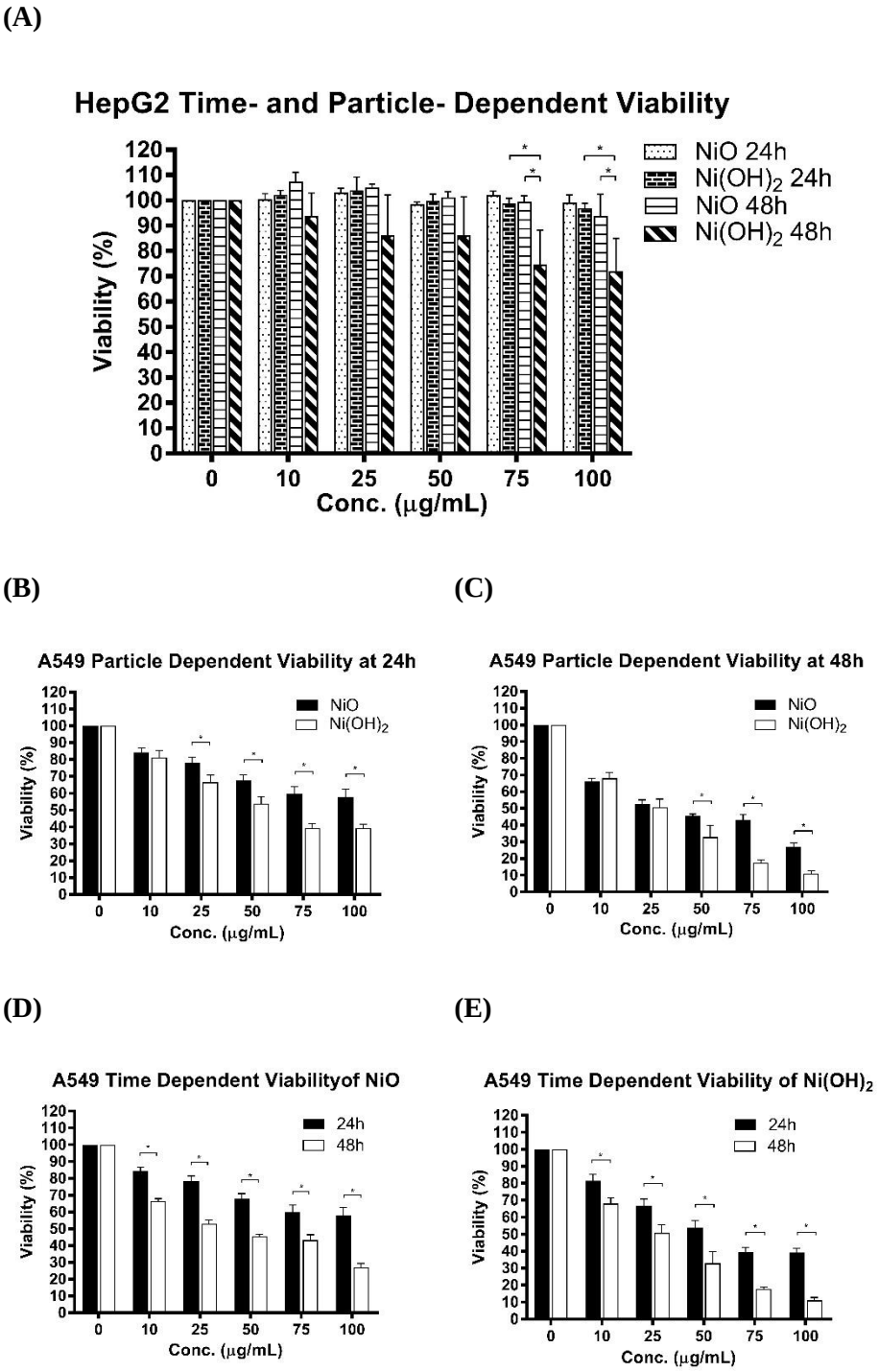

Figure 3. Cell viability upon exposure to NiO or $Ni(OH)_2$. (A) Viability of Hep-G2 cells upon exposure to NiO or $Ni(OH)_2$ at the time periods of 24h and 48h. Particle-dependent viability of NiO vs. $Ni(OH)_2$ is seen at the time periods of (B) 24h and (C) 48h. Time dependent-viability of 24h vs. 48h is shown for the particles (D) NiO and (E) $Ni(OH)_2$. N=3, *$p<0.05$ vs control using a one-way ANOVA test followed by Tukey post hoc test.

(24h) and 11.1% (48h) at 100 µg/mL. Overall, reduction in viability occurred in a NP concentration-dependent manner. Importantly, cells tested at 48h had a steeper decrease in viability than cells exposed to the same NP for 24h. Due to the significant differences in toxicity upon NiO or $Ni(OH)_2$ exposure, A549 cells were subject to subsequent mechanistic studies of cytotoxicity.

3.3. OXIDATIVE STRESS

3.3.1. Elevation of Oxidative Stress (OS). Oxidative stress was measured upon NiO or $Ni(OH)_2$ exposure in A549 cells to determine its role in the decrease of cell viability. At 24h, both NPs increased OS at 25 µg/mL and above, with $Ni(OH)_2$ producing a steeper increase of OS ($N=4$, $p<0.05$). At 100 µg/mL, OS was elevated up to 1.7 and 2.5-fold by NiO and $Ni(OH)_2$, respectively. A strong positive linear correlation existed between OS and viability for both NiO ($R^2 = 0.93$) and $Ni(OH)_2$ ($R^2 = 0.98$) at 24h (Appendix A2). At 48h, NiO significantly increased OS at 25 µg/mL and above while $Ni(OH)_2$ increased ROS at all tested concentrations ($N=4$, $p<0.05$). Distinctively, NiO induced OS at a much steeper increase than $Ni(OH)_2$ at 48h (Fig, 4). OS was increased by up to 4.3 and 3.3 times in NiO and $Ni(OH)_2$, respectively. Regardless of the fold increase, a strong positive linear correlation existed between OS and viability for both NiO ($R^2 = 0.95$) and $Ni(OH)_2$ ($R^2 = 0.99$) at 48h (Appendix A2).

3.3.2. Perturbation of Mitochondrial Membrane Potential (MMP). The dissipation of mitochondrial membrane potential was observed to determine its role in loss of viability in A549 cells upon exposure to NiO or $Ni(OH)_2$. In the untreated control cells, an abundance of red color is indicative of healthy mitochondria. Cells treated with

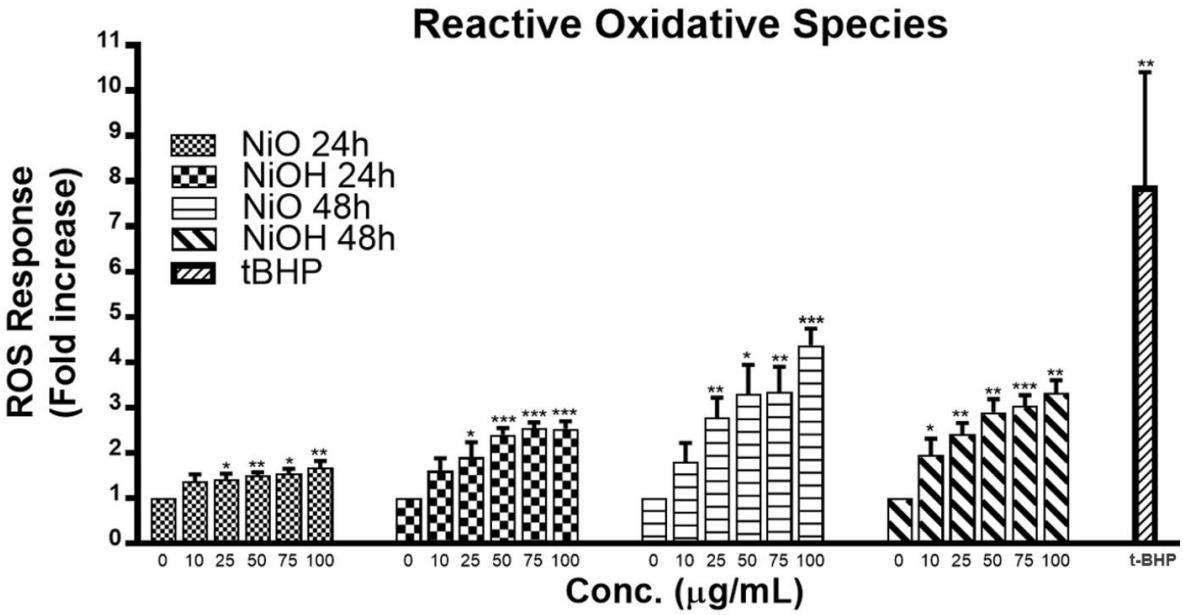

Figure 4. ROS produced in A549 cells upon exposure to NiO or $Ni(OH)_2$. *p<0.05 vs control using a one-way t- test. **p<0.01. ***p<0.001. N=4.

$Ni(OH)_2$ or NiO experience OS and have a noticeable decrease in healthy mitochondria (Fig 5). Exposure to $Ni(OH)_2$ appears to decrease the abundance of healthy mitochondria more than exposure to NiO. This is likely a result of a higher OS production upon exposure to $Ni(OH)_2$, inducing a greater dissipation in MMP (Fig. 4). There seems to be little to no difference between 12h and 24h in NiO or $Ni(OH)_2$ exposed cells.

3.3.3. Elevation of Caspase-3 Enzymatic Activity. Caspase-3 enzymatic activity was measured to determine the role of programed cell death in A549 cells upon exposure to NiO or $Ni(OH)_2$ (Fig. 6). Exposure to NiO significantly increased caspase-3 activity in all groups except for 10 µg/mL at 24h and 48h (N=3, p<0.05). Caspase-3 enzymatic activity reached its highest level in NiO exposed cells at 75 µg/mL (1.40 fold) and 100 µg/mL (1.85 fold) after 24h and 48h exposure, respectively. $Ni(OH)_2$ also

significantly increased caspase-3 activity in all exposed groups at 24h and 48h (N=3, $p<0.05$).

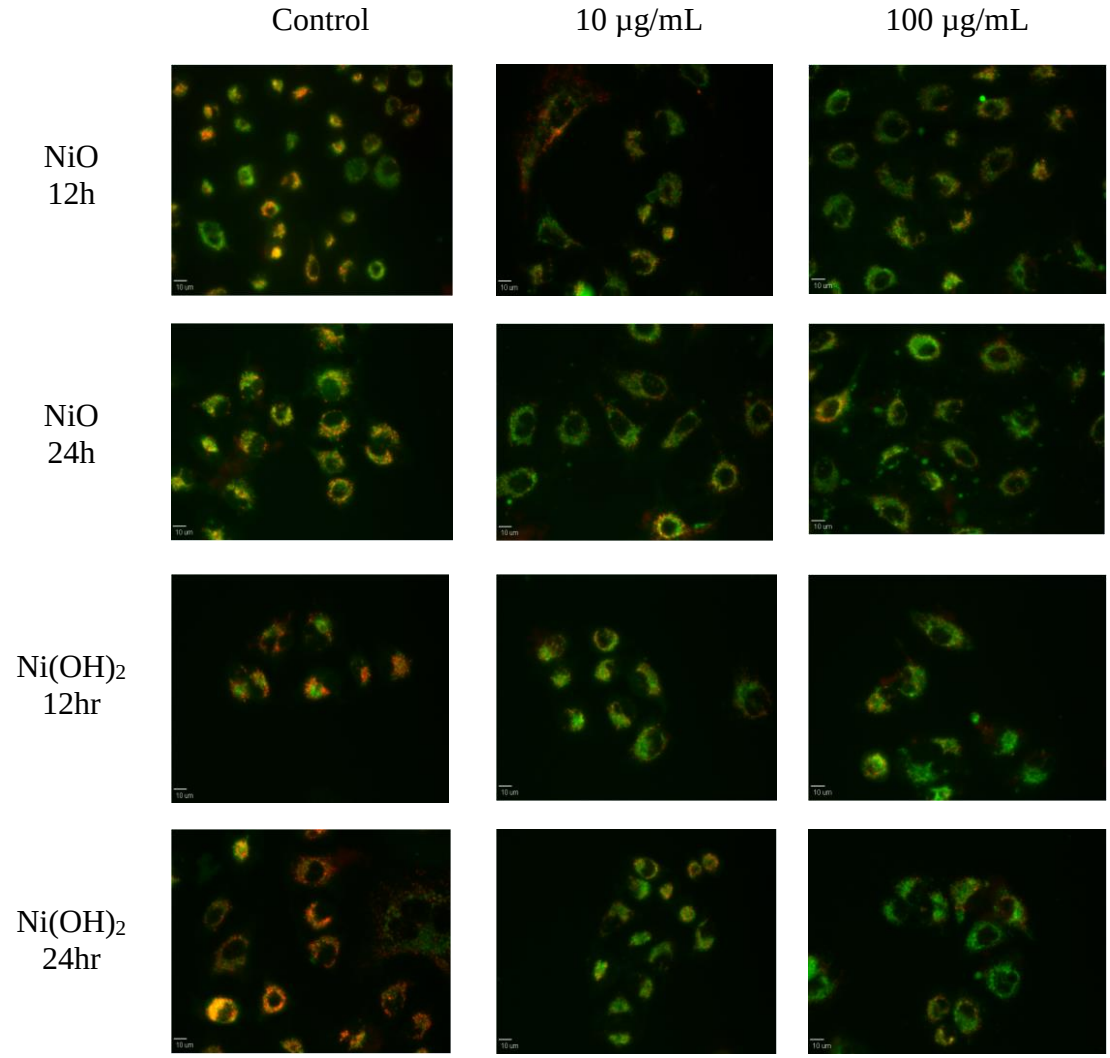

Figure 5. Fluorescence microscopy images of mitochondria membrane potential after exposure to NiO or $Ni(OH)_2$ for 12h or 24h.

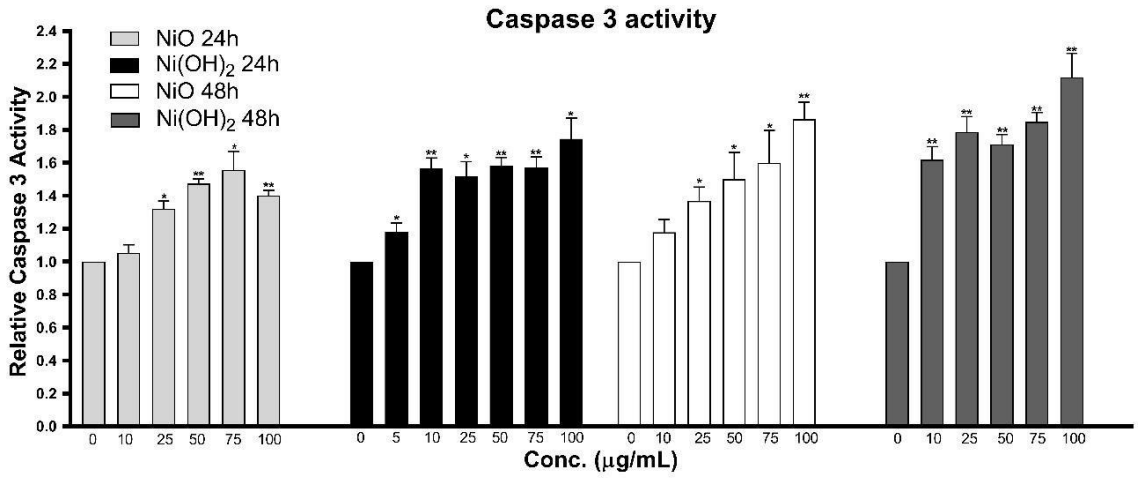

Figure 6. Measurement of Caspase-3 activity after exposure of NiO or $Ni(OH)_2$ to A549 cells at 10, 25, 50, 75, and 100 µg/mL relative to the control. *p<0.05 vs. % of control using a one-way t-test. **p<0.01. N=3.

Exposure to 100 µg/mL of $Ni(OH)_2$ increased caspase-3 enzymatic activity by 1.7 and 2.1 times 24h and 48h, respectively.

3.3.4. Cell Death – Apoptosis. Apoptosis was measured to determine the role of programed cell death in viability in A549 cells upon NiO or $Ni(OH)_2$ exposure (Fig. 7). For our purpose, the total apoptotic percentage of each population was the summation of the subpopulation of cells undergoing early apoptosis and late apoptosis. Exposure to NiO significantly increased the percentage of cells undergoing apoptosis at 50, 75, and100 µg/mL at 24h, reaching up to 9.8% (N=4, p<0.05). Exposure to NiO significantly increased the percentage of cells undergoing apoptosis at 25 and 100 µg/mL at 48h (N=4, p<0.05). Interestingly, the rate of apoptosis decreased from 10.6% (at 25 µg/mL) to 7.3% (at 50 µg/mL) and 6.4 (at 75 µg/mL) before once again increasing to 9.8% (at 100 µg/mL). Exposure to $Ni(OH)_2$ significantly increased the percentage of cells undergoing

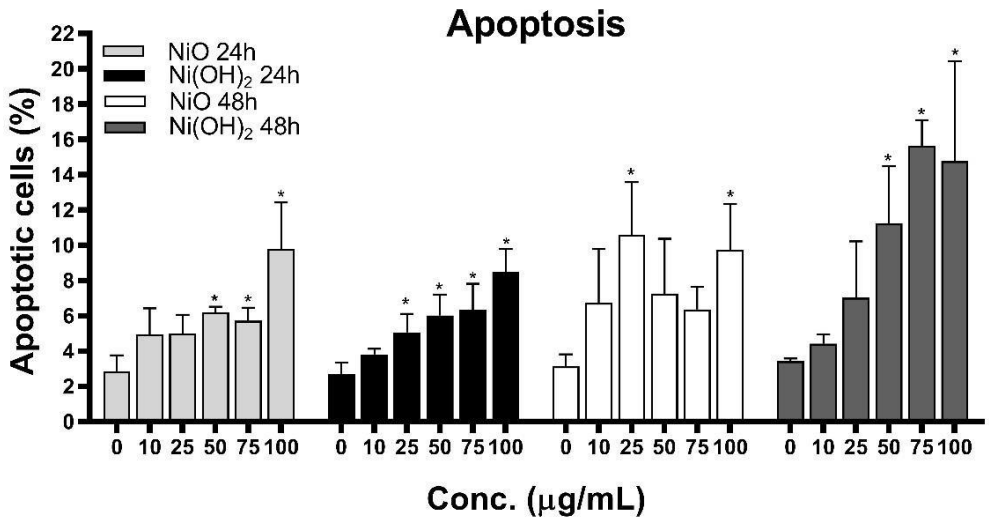

Figure 7. Flow cytometer analysis of apoptosis in A549 cells after exposure to NiO or $Ni(OH)_2$ for 24 or 48 hours. *$p < 0.05$ compared to each respective control using a one-way ANOVA with a Dunnett comparison.

apoptosis at 25 μg/mL and above at 24h and at 50 μg/mL and above at 48h (N=4, $p<0.05$). Apoptotic percentages reached up to 8.5% and 14.7% for 24h and 48h $Ni(OH)_2$ exposure, respectively.

3.4. ALTERATION OF CELL CYCLE LEADS TO A SUPRESSION OF PROLIFERATION

3.4.1. Alteration of Cell Cycle. The alteration of cell cycle was measured in A549 cells upon exposure to NiO or $Ni(OH)_2$ to determine whether cells become arrested in various phases of the cell cycle. Cells can become arrested in any phase of the cell cycle depending on various regulatory factors. Exposure to NiO and $Ni(OH)_2$ resulted in different changes in the cell cycle (Fig. 8). Cells were arrested in the S phase upon 24h NiO exposure while cells became arrested in the S and G2/M phase upon 24h $Ni(OH)_2$

exposure. After 24h, cells in the S phase increased by 6.9% and 5.1% Upon NiO and $Ni(OH)_2$ exposure, respectively. The percentage of cells in the G2/M phase decreased upon 24h NiO exposure by 2.6% and increased upon 24h $Ni(OH)_2$ exposure by 2.4%. After 48h, cells in the S phase increased by 2.3% and 4.5% Upon NiO and $Ni(OH)_2$ exposure, respectively. The percentage of cells in the G2/M phase decreased upon 24h NiO exposure by 2.2% and increased upon 24h $Ni(OH)_2$ exposure by 11.5%.

3.4.2. Suppression of Cellular Proliferation. Proliferation was measured to determine its role in cellular viability in A549 Comparisons in inhibition of proliferation are hard to determine from the cell cycle results because the cells became arrested in different phases (Fig. 9). Exposure to NiO or $Ni(OH)_2$ significantly reduced the rate of proliferation at all tested concentrations at both time points ($N=4$, $p<0.05$). A steady decrease in proliferation was seen at each increasing concentration of NP at 24h. NiO and $Ni(OH)_2$ reduced proliferation to 46.1% and 27.1%, respectively at the highest tested concentration (100 µg/mL). There was as strong positive linear relationship between viability and proliferation for NiO ($R^2 = 0.97$) and $Ni(OH)_2$ ($R^2 = 0.96$) at 24h (Appendix A5). Increasing concentrations of NiO resulted in a steady decrease in proliferation at 48h, dropping the proliferation rate to 21.6% at 100 µg/mL. $Ni(OH)_2$ exposure at 48h produced a steep decrease in proliferation between 25 µg/mL and 50 µg/mL. Proliferation rates dropped from 47.2% (at 25 µg/mL) to 13.7% (at 50 µg/mL) and ultimately down to 4.4% (at 100 µg/mL). There was as strong positive linear

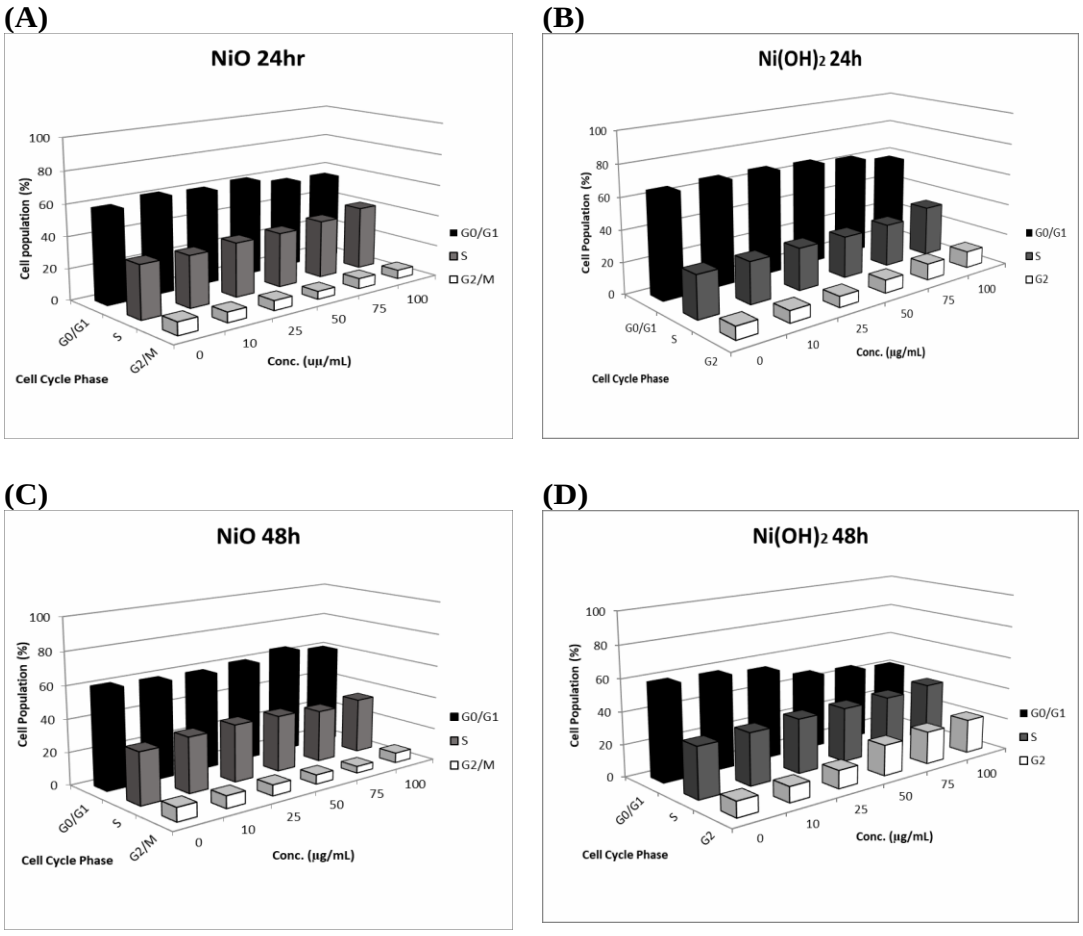

Figure 8. Flow cytometer analysis of cell cycle of A549 cells. Analysis was measured after exposure to (A) 24h NiO (B) 24h $Ni(OH)_2$, (C) 48h NiO (D) 48h $Ni(OH)_2$.

relationship between viability and proliferation for NiO ($R^2 = 0.92$) and $Ni(OH)_2$ ($R^2 = 0.98$) at 48h (Appendix A5).

4. DISCUSSION

In this study, we investigated the comparative cytotoxicity of two nickel NPs and explored several cellular responses as components of cytotoxicity. We hypothesized that

1) cytotoxicity of NiO and $Ni(OH)_2$ NPs is cell line-, particle-, time-, and dose-dependent, 2) cytotoxicity is mediated by oxidative stress and subsequent cellular events

Table 2. Changes in percentage of cells in various phases of the cell cycle upon exposure to NiO or $Ni(OH)_2$ for 24h or 48h.

	G_0/G_1	S	G_2/M
24h NiO	-2.9	+6.9	-2.6
24h $Ni(OH)_2$	-7.7	+5.1	+2.4
48h NiO	0	+2.3	-2.2
48h $Ni(OH)_2$	-17	+5.4	+11.5

including modulation of mitochondrial membrane potential and caspase-3 enzyme activity, and 3) exposure to NiO and $Ni(OH)_2$ NPs alters cell cycle leading to suppression of cell proliferation. Cell viability assays revealed that cytotoxicity is cell line-dependent. A549 cells (a lung cell line) are much more sensitive to NPs than HepG2 cells (a liver cell line). As A549 cells are epithelial cells in a respiratory organ, it is presumably to be more sensitive to particle exposure than hepatic cells. Other studies are in agreement with this notion. For instance, A549 cells experienced greater induction of OS and lactate dehydrogenase (LDH) leakage, reduction in glutathione (GSH) levels, dissipation of MMP, elevation of apoptotic gene expression, and decline in cellular viability than HepG2 cells upon exposure to $CuFe_2O_4$ and $ZnFe_2O_4$ NPs [30, 31]. Upon

exposure to a variety of sizes and concentrations of silica NPs, HepG2 cells are less susceptible than A549 to toxic responses, including ROS induction, decline in GSH, and

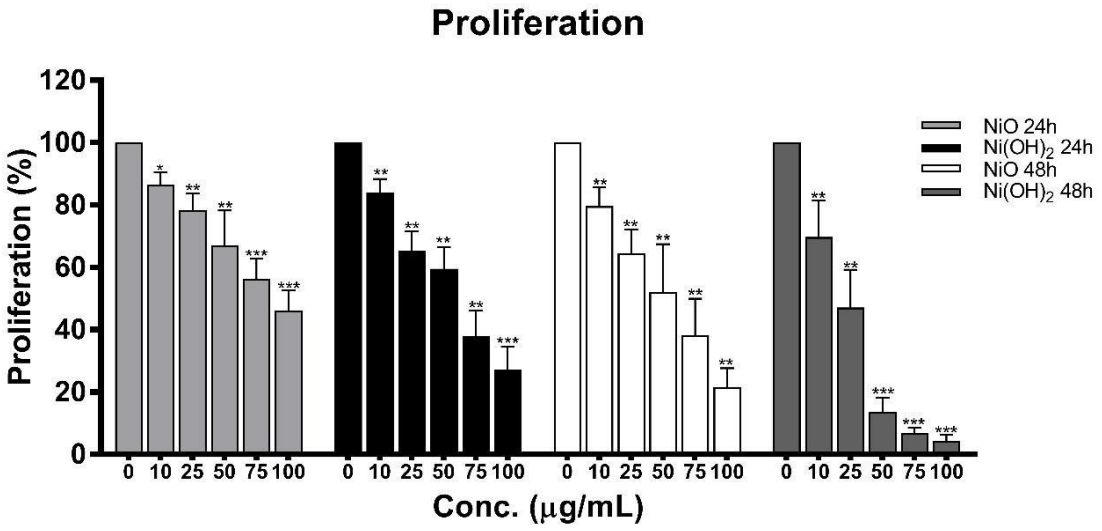

Figure 9. Inhibition of proliferation of A549 cells upon exposure to NiO or $Ni(OH)_2$. *p<0.05 vs. control using a one-way t-test. **p<0.01. ***p<.0001. N=4.

reduction of cell viability [32]. A549 cells experienced a greater reduction in MMP and reduction of viability than HepG2 cells upon silver NP exposure [33]. Another possible explanation regarding the discrepancy of in vitro toxic response may be due to the fact that the liver has a higher capacity of detoxifying functions (i.e., phase I & II enzymes) than the lung. In vivo comparisons may also need to consider translocation of NPs from the lung to the liver [34, 35].

We found that NiO and $Ni(OH)_2$-induced cytotoxicity is concentration-, time-, and particle-specific in A549 cells. A549 cells experienced concentration-dependent

viability in all tested concentrations. Our studies were in agreement with other studies, who further demonstrated that BEAS-2B cells are 1.5-fold more sensitive than A549 to NiO [20, 21, 36]. While there are no studies of $Ni(OH)_2$ toxicity in human cells, one study did find concentration-dependent viability of $Ni(OH)_2$ in the modified CHO-K1 cell line AS52 [28]. Our data revealed time- and particle- dependent cell viability of NiO and $Ni(OH)_2$ in A549 cells. Previous studies also found particle-dependent toxicity between different nickel NPs. NiO NPs were found to induce more DNA damage than Ni metal NPs in A549 cells [37]. The LC50 of NiOH is more than 6 times higher than that of black NiO in the modified Chinese Hamster Ovary cell AS52 [28]. Further studies are needed to determine the reason behind particle-dependent toxicity.

Our concentration- and time-dependent studies revealed dynamic changes in OS-induced cellular injuries as well as alteration of cell cycle leading to various degrees of suppression of cell proliferation. OS was elevated upon exposure to NiO and $Ni(OH)_2$ and had a strong correlation with cell viability at both time points. This informs that the generation of free radicals and oxidants is a hallmark of NP toxicity that triggers consequential molecular events leading to cell death. OS-mediated dissipation of MMP due to exposure to both NPs was supported by apparent reduction in influx of cationic JC-1 into mitochondria. Reduction of the number of healthy mitochondria in a cell might play a consequential role in perturbing homeostasis of bioenergetics and multiple signaling pathways pertaining to cell survival. One such signaling alteration is caspase-3 enzymatic activity and subsequent apoptosis. In general, our data indicates both NiO and $Ni(OH)_2$ elevates apoptosis in a time- and concentration-dependent manner, although the trend is atypical. A review on literature revealed the complexity of NP-induced cell

death. NiO-induced apoptosis in A549 cells did not elevate in a concentration-dependent manner similar to the trend seen in our 48h NiO apoptosis results [21]. This study also measured necrosis and found a consistent concentration-dependent increase. Another study found that Mn_2O_3-induced apoptosis in A549 cells increased in various increments [29]. The apoptotic rate would stay relatively the same between two concentrations before drastically increasing in a subsequent concentration. By contrast, PVP-coated Ag and Ag^+ NPs induced both apoptosis and necrosis in time- and particle-dependent manners in THP-1 monocyte cells [38]. The roles of apoptosis and necrosis are dynamic in the context of acute response and prolonged exposure.

The degree of cell viability imposed by exposure to NPs is a function of cell death and cell proliferation. As cell death induced by NPs has been demonstrated by a wealth of literature, suppression of cell proliferation is relatively under-studied. Our tritiated thymidine incorporation indicates a very strong linear correlation between cell viability and proliferation for NiO and $Ni(OH)_2$ over a period of 48h. These correlations indicate that suppression of proliferation is a key factor in determining reduction of cell viability. Modulation of cell proliferation has multiple causations. Alteration of cell cycle is one of them. Our results showed that NiO arrests A549 cells in the S phase while $Ni(OH)_2$ arrests cells in the S and G2/M phase. Previous studies have also found NP-mediated, phase-specific alteration of cell cycle. Exposure to TiO2 caused HaCat cells to arrest in the S phase while ZnO and CuO exposure caused G2/M arrest [39-41]. NPs composed of the same elements but have different properties can also influence phase-specific arrest. TiO_2 arrested cells in the G2/M phase while arresting cells in the G0/G1 phase [42-44].

Mechanisms of action that dictate particle- and phase-specific cell cycle alteration remain unclear.

5. CONCLUSION

We have demonstrated that toxicity exerts by NiO and $Ni(OH)_2$ NPs is cell line-concentration-, time-, and particle-dependent in the range of 10-100 µg/mL. $Ni(OH)_2$ is more cytotoxic than NiO. NP-induced oxidative stress triggered subsequent dissipation of mitochondrial membrane potential and induction of caspase-3 enzyme activity. The subsequent apoptotic events lead to reduction in cell number, though the contribution of necrosis to cell viability is unknown. In addition to cell death, suppression of cell proliferation contributes to plays an essential role in regulating cell number. Elevated OS had a strong correlation with viability. Collectively, the observed cell viability is a function of cell death and suppression of proliferation (Fig. 10)

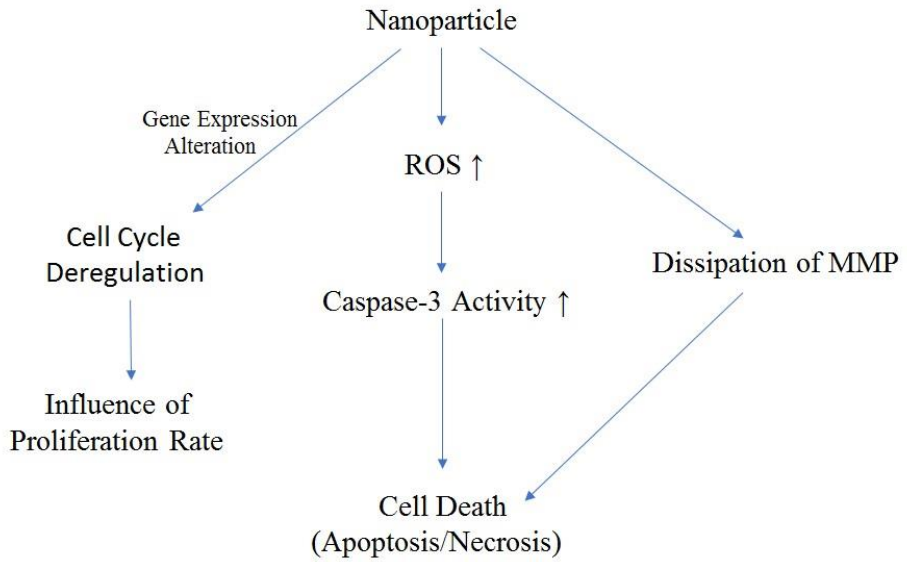

Figure 10. Cell viability is a function of cell death and suppression of proliferation.

REFERENCES

1. Nohynek, G. J.; Dofour, E. K.; Roberts, M. S., Nanotechnology, Cosmetics and the Skin: Is There a Health Risk? *Skin Pharmacology and Physiology* **2008,** 21, (3), 136-149.

2. Jong, W. H. D.; Borm, P., J., Drug Delivery and Nanoparticles; Applications and Hazards. *International Journal of Nanomedicine* **2008,** 3, (2), 133-149.

3. O'Neal, D. P.; Hirsch, L. R.; Halas, N. J.; Payne, J. D.; West, J. L., Photo-Thermal Tumor Ablation in Mice Using Near Infrared-Absorbing Nanoparticles. *Cancer Letters* **2004,** 209, (2), 171-6.

4. Kowshik, M.; Deshmukh, N.; Vogel, W.; Urban, J.; Kulkarni, S. K.; Paknikar, K. M., Microbial Synthesis of Semiconductor Cds Nanoparticles, their Characterization, and their use in the Fabrication of an Ideal Diode. *Biotechnology and Bioengineering* **2002,** 78, (5).

5. Weir, A.; Westerhoff, P.; Fabricius, L.; Hristovski, K.; von Goetz, N., Titanium Dioxide Nanoparticles in Food and Personal Care Products. *Environmental Science & Technology* **2012,** 46, (4), 2242-50.

6. Li, Y.; Wu, Y.; Ong, B. S., Facile Synthesis of Silver Nanoparticles Useful for Fabrication of High-Conductivity Elements for Printed Electronics. *Journal of the American Chemical Society* **2005,** 127, (10), 3266-3267.

7. Highsmith, J., Nanoparticles in Biotechnology, Drug Development and Drug Delivery. *Global Markets: A BCC Research Report* **2014**.

8. van Broekhuizen, P.; van Broekhuizen, F.; Cornelissen, R.; Reijnders, L., Workplace Exposure to Nanoparticles and the Application of Provisional Nanoreference Values in Times of Uncertain Risks. *Journal of Nanoparticle Research* **2012,** 14, (4).

9. Lai, X.; Wei, Y.; Zhao, H.; Chen, S.; Bu, X.; Lu, F.; Qu, D.; Yao, L.; Zheng, J.; Zhang, J., The Effect of Fe_2O_3 and ZnO Nanoparticles on Cytotoxicity and Glucose Metabolism in Lung Epithelial Cells. *Journal of Applied Toxicology : JAT* **2015,** 35, (6), 651-64.

10. Di Bucchianico, S.; Gliga, A. R.; Akerlund, E.; Skoglund, S.; Wallinder, I. O.; Fadeel, B.; Karlsson, H. L., Calcium-Dependent Cyto- and Genotoxicity of Nickel Metal and Nickel Oxide Nanoparticles in Human Lung Cells. *Particle and Fibre Toxicology* **2018,** 15, (1), 32.

11. Vamanu, C. I.; Cimpan, M. R.; Hol, P. J.; Sornes, S.; Lie, S. A.; Gjerdet, N. R., Induction of Cell Death by TiO_2 Nanoparticles: Studies on a Human Monoblastoid Cell Line. *Toxicology in Vitro* **2008,** 22, (7), 1689-96.

12. Han, J. W.; Gurunathan, S.; Jeong, J. K.; Choi, Y. J.; Kwon, D. N.; Park, J. K.; Kim, J. H., Oxidative Stress Mediated Cytotoxicity of Biologically Synthesized Silver Nanoparticles in Human Lung Epithelial Adenocarcinoma Cell Line. *Nanoscale Research Letters* **2014,** 9, (459).

13. Limbach, L. K.; Li, Y.; Grass, R. N.; Hintermann, M. A.; Muller, M.; Gumther, D.; Stark, W. J., Oxide Nanoparticle Uptake in Human Lung Fibroblasts: Effects of Particle Size, Agglomeration, and Diffusion at Low Concentrations. *Environmental Science & Technology* **2005,** 39, (23).

14. Martindale, J. L.; Holbrook, N. J., Cellular Response to Oxidative Stress: Signaling for Suicide and Survival. *Journal of Cellular Physiology* **2002,** 192, (1), 1-15.

15. Huang, Y. H.; Cambre, M.; Lee, H. J., The Toxicity of Nanoparticles Depends on Multiple Molecular and Physicochemical Mechanisms. *International Journal of Molecular Sciences* **2017,** 18, (12).

16. Jiang, J.; Oberdorster, G.; Elder, A.; Gelein, R.; Mercer, P.; Biswas, P., Does Nanoparticle Activity Depend upon Size and Crystal Phase? *Nanotoxicology* **2008,** 2, (1), 33-42.

17. Forest, V.; Leclerc, L.; Hochepied, J. F.; Trouve, A.; Sarry, G.; Pourchez, J., Impact of Cerium Oxide Nanoparticles Shape on Their in Vitro Cellular Toxicity. *Toxicology in Vitro* **2017,** 38, 136-141.

18. Baek, M.; Kim, M. K.; Cho, H. J.; Lee, J. A.; Yu, J.; Chung, H. E.; Choi, S. J., Factors Influencing the Cytotoxicity of Zinc Oxide Nanoparticles: Particle Size and Surface Charge. *Journal of Physics: Conference Series* **2011,** 304, 012044.

19. Kai, W.; Xiaojun, X.; Ximing, P.; Zhenqing, H.; Qiqing, Z., Cytotoxic Effects and the Mechanism of Three Types of Magnetic Nanoparticles on Human Hepatoma BEL-7402 Cells. *Nanoscale Research Letters* **2011,** 6, 480.

20. Chusuei, C. C.; Wu, C. H.; Mallavarapu, S.; Hou, F. Y.; Hsu, C. M.; Winiarz, J. G.; Aronstam, R. S.; Huang, Y. W., Cytotoxicity in the Age of Nano: The Role of Fourth Period Transition Metal Oxide Nanoparticle Physicochemical Properties. *Chemico-Biological Interactions* **2013,** 206, (2), 319-26.

21. Capasso, L.; Camatini, M.; Gualtieri, M., Nickel Oxide Nanoparticles Induce Inflammation and Genotoxic Effect in Lung Epithelial Cells. *Toxicology Letters* **2014,** 226, (1), 28-34.

22. AZoNano. Nickel Oxide (NiO) Nanoparticles—Properties, Applications. Available online: https://www.azonano.com/article.aspx?ArticleID=3378 (accessed on 21 October 2017).

23. Ugurlu, B. Nickel Hydroxide Nanoparticles and Usage Areas of Nickel Hydroxide Nanopowders. Available online: https://nanografi.com/blog/nickel-hydroxide- nanoparticles-and-usage-areas-of-nickel-hydroxide-nanopowders/ (accessed on July 2018).

24. Kadoya, C.; Ogami, A.; Morimoto, Y.; Myojo, T.; Oyabu, T.; Nishi, K.; Yamamoto, M.; Todoroki, M.; Tanka, I., Analysis of Bronchoalveolar Lavage Fluid adhering to lung surfacant. *Industrial Health* **2012,** 50, (31-36).

25. Kang, G. S.; Gillespie, P. A.; Chen, L. C., Inhalation Exposure to Nickel Hydroxide Nanoparticles Induces Systemic Acute Phase Response in Mice. *Toxicological Research* **2011,** 27, (1), 19-23.

26. Horie, M.; Fukui, H.; Nishio, K.; Endoh, S.; Kato, H.; Fujita, K.; Miyauchi, A.; Nakamura, A.; Shichiri, M.; Ishida, N.; Kinugasa, S.; Morimoto, Y.; Niki, E.; Yoshida, Y.; Iwhashi, H., Evaluation of Acute Oxidative Stress Induced by NiO Nanoparticles in Vivo and in Vitro. *Journal of Occupational Health* **2011,** 52, 31-36.

27. Siddiqui, M. A.; Ahamed, M.; Ahmad, J.; Majeed Khan, M. A.; Musarrat, J.; Al-Khedhairy, A. A.; Alrokayan, S. A., Nickel Oxide Nanoparticles Induce Cytotoxicity, Oxidative Stress and Apoptosis in Cultured Human Cells that is Abrogated by the Dietary Antioxidant Curcumin. *Food And Chemical Toxicology* **2012,** 50, (3-4), 641-7.

28. Fletcher, G. G.; Rossestto, F. E.; Turnbull, J. D.; Nieboer, E., Toxicity, Uptake, and Mutagenicity of Particulate and Soluble Nickel Compounds. *Environmental Health Perspectives* **1994,** 102, 69-79.

29. Chusuei, C. C.; Wu, C. H.; Mallavarapu, S.; Hou, F. Y.; Hsu, C. M.; Winiarz, J. G.; Aronstam, R. S.; Huang, Y. W., Cytotoxicity in the Age of Nano: The Role of Fourth Period Transition Metal Oxide Nanoparticle Physicochemical Properties Supplementary Information. *Chemico-Biological Interactions.*

30. Alhadlaq, H. A.; Akhtar, M. J.; Ahamed, M., Zinc Ferrite Nanoparticle-Induced Cytotoxicity and Oxidative Stress in Different Human Cells. *Cell & Bioscience* **2015,** 5, 55.

31. Ahmad, J.; Alhadlaq, H. A.; Alshamsan, A.; Siddiqui, M. A.; Saquib, Q.; Khan, S. T.; Wahab, R.; Al-Khedhairy, A. A.; Musarrat, J.; Akhtar, M. J.; Ahamed, M., Differential Cytotoxicity of Copper Ferrite Nanoparticles in Different Human Cells. *Journal Of Applied Toxicology* **2016,** 36, (10), 1284-93.

32. Kim, I. Y.; Joachim, E.; Choi, H.; Kim, K., Toxicity of Silica Nanoparticles Depends on Size, Dose, and Cell Type. *Nanomedicine* **2015,** 11, (6), 1407-16.

33. Xin, L.; Wang, J.; Fan, G.; Che, B.; Wu, Y.; Guo, S.; Tong, J., Oxidative Stress and Mitochondrial Injury-Mediated Cytotoxicity Induced by Silver Nanoparticles in Human A549 and HepG2 Cells. *Environmental Toxicology* **2016,** 31, (12), 1691- 1699.

34. Sadauskas, E.; Jacobsen, N. R.; Danscher, G.; Stoltenberg, M.; Vogel, U.; Larsen, A.; Kreyling, W.; Wallin, H., Biodistribution of Gold Nanoparticles in Mouse Lung Following Intratracheal Instillation. *Chemistry Central Journal* **2009,** 3, 16.

35. Buckley, A.; Warren, J.; Hodgson, A.; Marczylo, T.; Ignatyev, K.; Guo, C.; Smith, R., Slow Lung Clearance and Limited Translocation of Four Sizes of Inhaled Iridium Nanoparticles. *Particle and Fibre Toxicology* **2017,** 14, (1), 5.

36. Mohamed, K.; Zine, K.; Fahima, K.; Abdelfattah, E.; Sharifudin, S. M.; Duduku, K., NiO Nanoparticles Induce Cytotoxicity Mediated Through ROS Generation and Impairing the Antioxidant Defense in the Human Lung Epithelial Cells (A549): Preventive Effect of Pistacia Lentiscus Essential Oil. *Toxicology Reports* **2018,** 5, 480-488.

37. Latvala, S.; Hedberg, J.; Di Bucchianico, S.; Moller, L.; Odnevall Wallinder, I.; Elihn, K.; Karlsson, H. L., Nickel Release, ROS Generation and Toxicity of Ni and NiO Micro- and Nanoparticles. *PloS one* **2016,** 11, (7), e0159684.

38. Foldbjerg, R.; Olesen, P.; Hougaard, M.; Dang, D. A.; Hoffmann, H. J.; Autrup, H., PVP-Coated Silver Nanoparticles and Silver Ions Induce Reactive Oxygen Species, Apoptosis and Necrosis in THP-1 Monocytes. *Toxicology Letters* **2009,** 190, (2), 156-62.

39. Gao, X.; Wang, Y.; Peng, S.; Yue, B.; Fan, C.; Chen, W.; Li, X., Comparative Toxicities of Bismuth Oxybromide and Titanium Dioxide Exposure on Human Skin Keratinocyte Cells. *Chemosphere* **2015,** 135, 83-93.

40. Gao, F.; Ma, N.; Zhou, H.; Wang, Q.; Zhang, H.; Wang, P.; Hou, H.; Wen, H.; Li, L., Zinc Oxide Nanoparticles-Induced Epigenetic Change and G_2/M Arrest are Associated with Apoptosis in Human Epidermal Keratinocytes. *International Journal of Nanomedicine* **2016,** 11, 3859-74.

41. Luo, C.; Li, Y.; Yang, L.; Zheng, Y.; Long, J.; Jia, J.; Xiao, S.; Liu, J., Activation of Erk and p53 Regulates Copper Oxide Nanoparticle-Induced Cytotoxicity in Keratinocytes and Fibroblasts. *International Journal of Nanomedicine* **2014,** 9, 4763-72.

42. Moschini, E.; Gualtieri, M.; Gallinotti, D.; Pezzolato, E.; Fascio, U.; Camatini, M.; Mantecca, P., Metal Oxide Nanoparticles Induce Cytotoxic Effects on Human Lung Epithelial Cells A549. *Chemical Engineering Trans.* **2010,** 22.

43. Kansara, K.; Patel, P.; Shah, D.; Shukla, R. K.; Singh, S.; Kumar, A.; Dhawan, A., TiO_2 Nanoparticles Induce DNA Double Strand Breaks and Cell Cycle Arrest in Human Alveolar Cells. *Environmental and Molecular Mutagenesis* **2015,** 56, (2), 204-17.

44. Wang, Y.; Cui, H.; Zhou, J.; Li, F.; Wang, J.; Chen, M.; Liu, Q., Cytotoxicity, DNA Damage, and Apoptosis Induced by Titanium Dioxide Nanoparticles in Human Non-Small Cell Lung Cancer A549 Cells. *Environmental Science and Pollution Research International* **2015,** 22, (7), 5519-30.

APPENDIX

ADDITIONAL FIGURES AND TABLES FROM PAPER II

Table A1. Number of cells used in each type of experiment.

Experiment	Plate used	Cells Seeded (24h)	Cells Seeded (48h)
SRB (A549), Proliferation, Caspase-3	24 well plate	45,000	22,000
SRB(HepG2)	24 well plate	120,000	120,000
Cell cycle, Apoptosis	6 cm plate	250,000	120,000
ROS	96 well plate	1,500	750
MMP	35 mm microscope plate	15,000	---

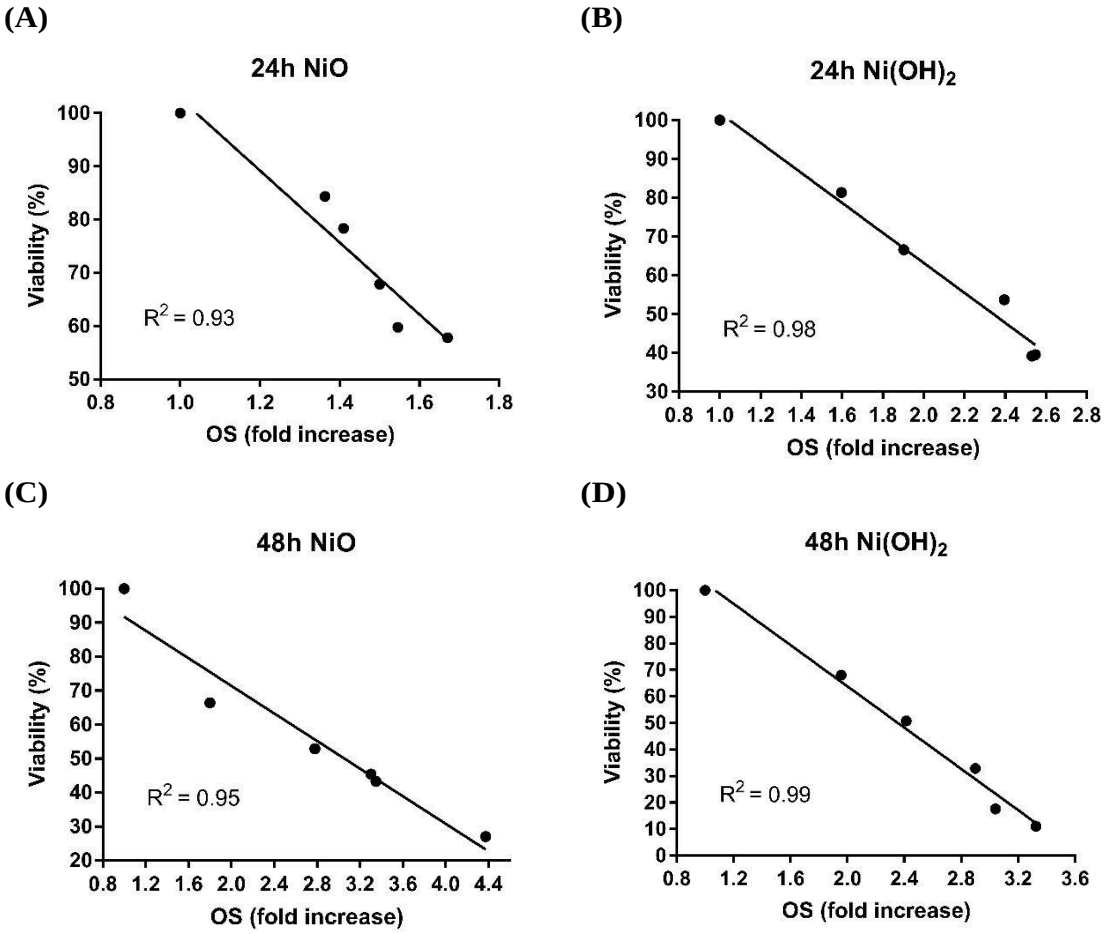

Figure A2. Linear correlation between viability and OS for (A) 24h NiO (B) 24h NiOH (C) 48h NiO (D) 48h NiOH.

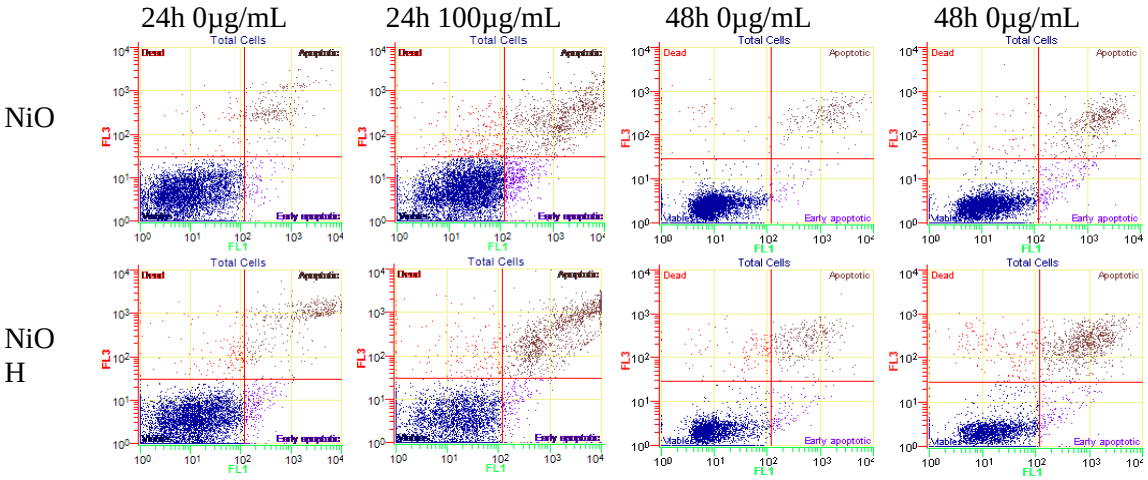

Figure A3. Apoptosis graphs.

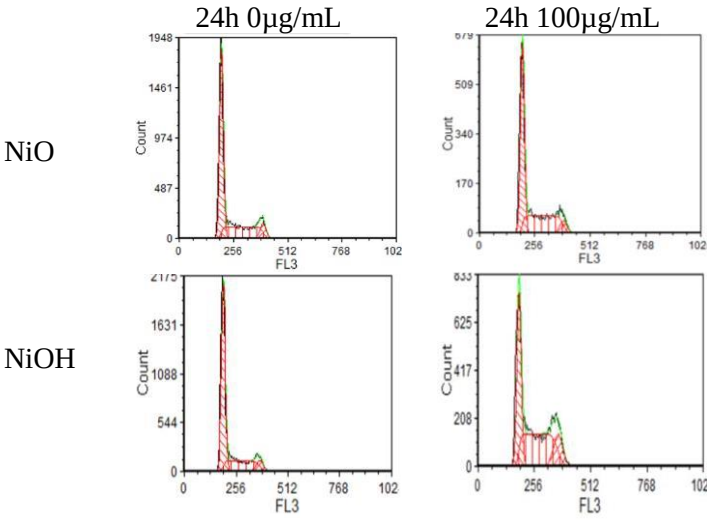

Figure A4. Cell cycle.

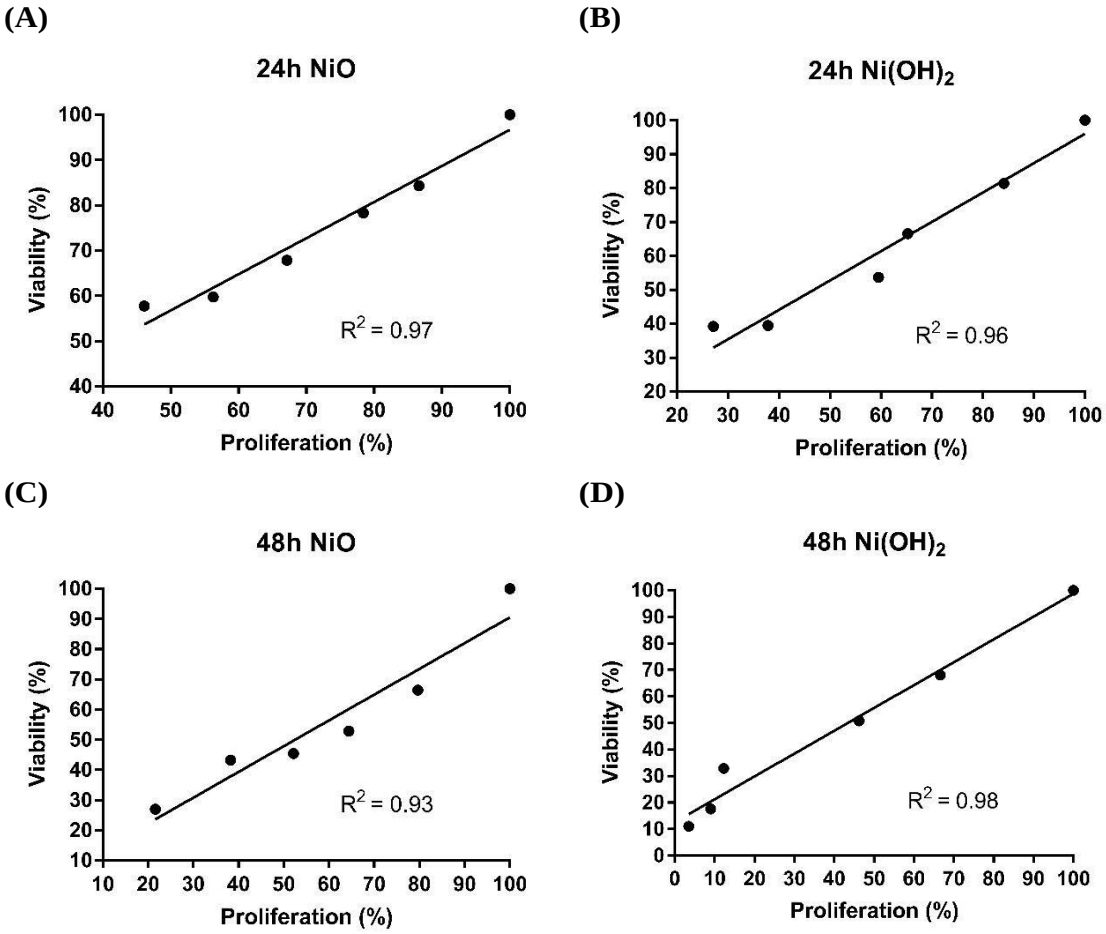

Figure A5. Linear correlation between viability and proliferation for (A) 24h NiO (B) 24h NiOH (C) 48h NiO (D) 48h NiOH.

SECTION

2. CONCLUSION

Recent studies have begun assessing the safety of nanoparticles to insure human and environmental health. Paper one explored some of the specific properties related to nanoparticle toxicity and have found size, surface area, shape, particle charge, dissolution rate, and available binding sites correlate with toxicity. The biochemical and molecular mechanisms of cytotoxicity were then explored, with an emphasis on the mechanisms of cell cycle alteration. Overall, viability is thought to be a function of the suppression of proliferation and cell killing. Paper two explored the specific differential toxicity between NiO and $Ni(OH)_2$. Differences in viability upon nanoparticle exposure were found to be cell line-, time-, concentration-, and particle-dependent. Various mechanisms responsible for viability were investigated including induction of oxidative stress, dissipation of mitochondrial membrane potential, and induction of caspase-3 enzymatic activity. Alterations in cell cycle, changes in proliferation rate, and induction of apoptosis were also delineated. In summary, cytotoxicity is mediated by oxidative stress-mediated cell death and suppression of proliferation.

VITA

Melissa Hope Cambre graduated from Lee's Summit North High School in Lee's Summit, MO in 2011. She graduated from Missouri University of Science and Technology in May of 2015 with a B.S. in Biological Sciences. She received her Master of Science in Applied and Environmental Biology degree from Missouri University of Science and Technology in December 2018.